Application of Fragment-Based Lead Generation to the Discovery of Novel, Cyclic Amidine β-Secretase Inhibitors with Nanomolar Potency, Cellular Activity, and High Ligand Efficiency[§]

Philip D. Edwards,*[,†] Jeffrey S. Albert,[†] Mark Sylvester,[†] David Aharony,[†] Donald Andisik,[†] Owen Callaghan,[+] James B. Campbell,[†] Robin A. Carr,[+] Gianni Chessari,[+] Miles Congreve,[+] Martyn Frederickson,[+] Rutger H. A. Folmer,[‡] Stefan Geschwindner,[‡] Gerard Koether,[†] Karin Kolmodin,[‡] Jennifer Krumrine,[†] Russell C. Mauger,[†] Christopher W. Murray,[+] Lise-Lotte Olsson,[‡] Sahil Patel,[+] Nate Spear,[†] and Gaochao Tian[†]

CNS Discovery Research, AstraZeneca Pharmaceuticals LP, 1800 Concord Pike, PO Box 15437, Wilmington, Delaware 19850-5437, Global Structural Chemistry, AstraZeneca, S-431 83 Mölndal, Sweden, and Astex Therapeutics Ltd, 436 Cambridge Science Park, Milton Road, Cambridge CB4 0QA, United Kingdom

Received July 9, 2007

Fragment-based lead generation has led to the discovery of a novel series of cyclic amidine-based inhibitors of β-secretase (BACE-1). Initial fragment hits with an isocytosine core having millimolar potency were identified via NMR affinity screening. Structure-guided evolution of these fragments using X-ray crystallography together with potency determination using surface plasmon resonance and functional enzyme inhibition assays afforded micromolar inhibitors. Similarity searching around the isocytosine core led to the identification of a related series of inhibitors, the dihydroisocytosines. By leveraging the knowledge of the ligand-BACE-1 recognition features generated from the isocytosines, the dihydroisocytosines were efficiently optimized to submicromolar potency. Compound **29**, with an IC_{50} of 80 nM, a ligand efficiency of 0.37, and cellular activity of 470 nM, emerged as the lead structure for future optimization.

Introduction

Alzheimer's disease (AD[a]) is a devastating disease affecting approximately 4.5 million individuals in the US.[1] AD primarily affects individuals over 60, and as the baby boomers age, the percentage of the population afflicted with AD will increase, with recent estimates suggesting that by 2050 as many as 16 million Americans will be afflicted.[1] In addition to the individual suffering and financial cost of AD, the impact on the families of those with AD is also significant. One in 10 Americans report having a family member with AD, and 7 out of 10 AD patients live at home.[2]

Consequently, the need to develop drugs to treat AD is a high priority in both academia and the pharmaceutical industry, with most major pharmaceutical companies having active AD programs. Currently, there are only two classes of drugs approved for treating AD.[3] Several acetylcholine esterase inhibitors have been on the market for a number of years and improve cognition by increasing synaptic levels of acetylcholine. Recently, a new drug has been approved, memantine, which is believed to improve cognition by controlling levels of glutamate via antagonism of the NMDA receptor. However, these drugs only treat the symptomology of AD and do not address the underlying neuropathology.

The most widely held hypothesis for the pathogenesis of Alzheimer's disease is that mismetabolism of amyloid precursor protein (APP) generates β-amyloid (Aβ) fibrils that aggregate to form neurofibrillary plaques, one of the morphological hallmarks of AD.[4] These Aβ fibrils and plaques interact directly with neurons initiating neurodegeneration leading to dementia. Two proteases are responsible for the proteolytic processing of APP: β-secretase and γ-secretase.[5] β-Secretase (BACE-1) is a membrane-associated aspartyl protease and cleaves the membrane-bound APP at an extramembrane site.[6−9] Subsequent to β-secretase cleavage, γ-secretase, a member of a unique class of intramembrane aspartyl proteases cleaves the C99 fragment generated from APP by BACE-1 at an intramembrane site, generating Aβ and releasing it from the membrane. Since β-secretase cleavage of BACE-1 is the rate-controlling step in APP processing to Aβ, it is considered a leading target for treating AD via control of Aβ release and deposition, and a major effort has been directed to identify β-secretase inhibitors.

Over the past decade, a large number of peptidic and pseudo-peptidic BACE-1 inhibitors have been reported.[10−15] The vast majority of these possess a hydroxyl group that displaces an active-site water molecule and forms hydrogen bonding interactions with the catalytic aspartates.[16−25] A seminal report by Ghosh and Tang described the X-ray crystal structure of a large peptidic inhibitor (OM99-2, **1**, Figure 1) complexed to BACE-1[26] and paved the way for structure-based design approaches to the development of BACE-1 inhibitors. While OM99-2 is a very potent BACE-1 inhibitor, its large size makes it unattractive for drug development, especially for CNS diseases for which the drug needs to penetrate the blood−brain barrier.[27,28] Ligand efficiency (LE) has been recently introduced as a means of assessing a compound's potency relative to its size.[29] In this report, we define LE as the free energy of binding divided by the heavy atom count (HAC), $LE = -\Delta G/HAC \approx -RT \ln(IC_{50})/HAC$. If we consider as a target for a drug candidate a molecular weight of <500 and an IC_{50} <10 nM, it can readily

[§] Coordinates for the β-secretase complexes with compounds **8c**, **24**, and **27** have been deposited in the Protein Data Bank under accession codes 2va5, 2va6, and 2va7, together with the corresponding structure factor files.

* To whom correspondence should be addressed. Phone: 302-886-8371; fax 302-886-5382; e-mail: philip.edwards@astrazeneca.com.

[†] AstraZeneca CNS Discovery Research.

[‡] AstraZeneca Global Structural Chemistry.

[+] Astex Therapeutics Ltd.

[a] Abbreviations. Aβ, beta-amyloid; ACN, acetonitrile; AD, Alzheimer's disease; APP, amyloid precursor protein; BACE-1, β-site APP cleaving enzyme; n-BuLi; n-butyllithium; CDI, 1,1′-carbonyldiimidazole; DMF, dimethylformamide; DCM, dichloromethane; EtOAc, ethyl acetate; EtOH, ethanol; FRIT, fragment hit; HCl, hydrochloric acid; LE, ligand efficiency; MeOH, methanol; MeI, methyl iodide; NaCl, sodium chloride; NaH, sodium hydride; SFC, supercritical fluid chromatography; TEA, triethylamine; TFA, trifluoroacetic acid; THF, tetrahydrofuran.

10.1021/jm070829p CCC: $37.00
Published on Web 11/07/2007

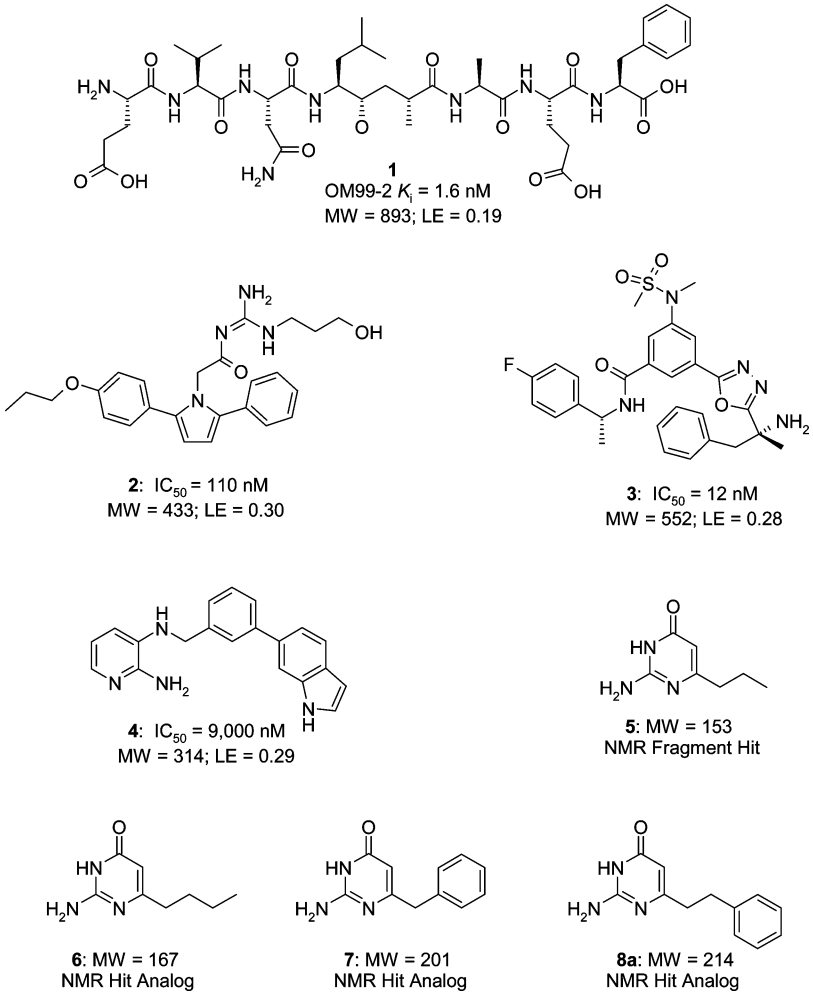

Figure 1. Examples of previously reported peptidic (**1**) and nonpeptidic (**2**−**4**) BACE-1 inhibitors, and initial fragment hits **5**−**8**.

be derived that an LE of >0.3 is desired. By comparison, the peptidic inhibitor OM99-2 (MW = 893, K_i = 1.6 nM) has an LE of only 0.19.[30]

While the vast majority of reported BACE-1 inhibitors are peptidic or pseudopeptidic, a number of reports have emerged revealing BACE-1 inhibitors with little or no peptidic character.[31−35] Particularly noteworthy are two recent reports of nonpeptidic BACE-1 inhibitors that possess novel functionality for interacting with aspartyl proteases. Cole et al. have described a series of acyl guanidines (**2**) in which the guanidine group interacts with the catalytic aspartates.[36] Rajapakse et al. have reported a series of oxadiazole BACE-1 inhibitors (**3**) in which the nitrogens of the oxadiazole ring form hydrogen bonds to the flap region of BACE-1.[37] These inhibitors represent significant advances in the development of nonpeptidic, drug-like BACE-1 inhibitors and possess moderate to good LE.

Previously, we revealed the discovery of a novel series of 2-aminopyridine BACE-1 inhibitors, **4**, using high throughput crystallographic screening.[38,39] In an accompanying paper in this journal issue, we reported the identification and characterization of a related series of isocytosine-based inhibitors, **5**, using NMR and other biophysical techniques.[40] Similarity searching of our corporate compound collection led to screening of compounds **6**−**8a**, with **8a** emerging as the lead isocytosine fragment hit. Herein, we describe the optimization of the isocytosine inhibitors and disclose the discovery of a novel series of dihydroisocytosines that possess nanomolar potency, excellent LE, and cellular activity.

Chemistry

The synthesis of the isocytosine analogues is outlined in Scheme 1. Condensation of a β-ketoester **9** with guanidine afforded the 6-substituted isocytosines **8**.[41] Methylation of the N^3 nitrogen was effected with MeI.[42] In the case of the isocytosines, methylation occurred predominantly on the N^3 nitrogen. Minor amounts of other methylated products were readily removed by chromatography. Preparation of the biphenyl analogues **11** was achieved via Suzuki coupling of bromide **10e**.

Preparation of the dichlorophenyl dihydroisocytosine derivatives entailed condensation of the α,β-unsaturated esters **12** with guanidine[43] (Scheme 2). Protection of the exocyclic amino group of **13d** as the *N*,*N*-dimethylformamidine,[44] methylation with MeI followed by deprotection with methanolic ammonia[44] afforded the N^3-methyldihydroisocytosine **16**. In contrast to the isocytosines, the dihydroisocytosines required the protection step to avoid significant amounts of undesired methylation products.

Application of the above route to the construction of other 6-substituted dihydroisocytosines proved to be limited because of the generation of large amounts of unwanted mono- and polymethylated side products during the methylation step. Consequently, we developed a synthesis in which the N^3-methyl group was regiospecifically incorporated prior to construction of the dihydroisocytosine ring system (Scheme 3). The lynchpin for this route was the α,β-unsaturated *N*-methylcyanamide **20**,[45] wherein the *N*-methyl substituent is ultimately transformed into the N^3-methyl group. Michael addition of methoxybenzylamine to **20**, followed by intramolecular cyclization yielded the desired

Scheme 1. Synthesis of Isocytosines **8**, **10**−**11**[a]

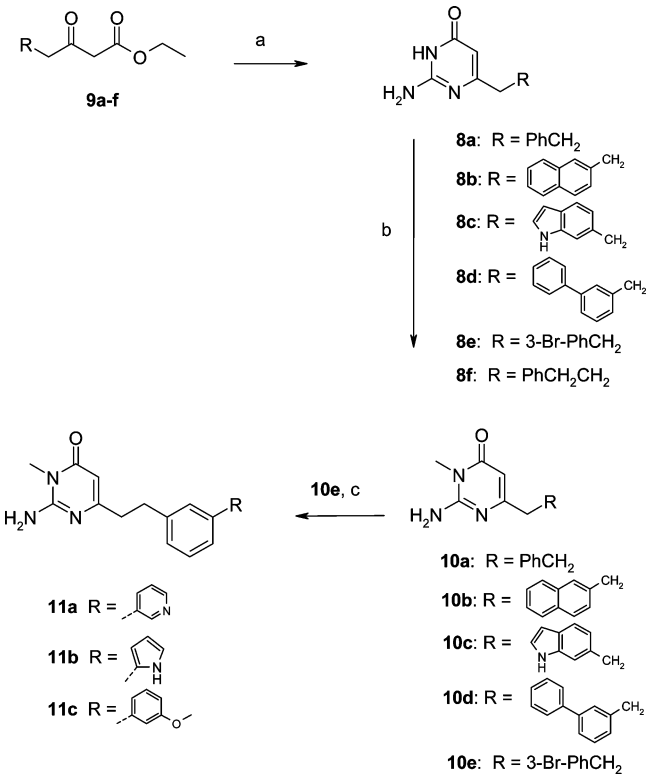

[a] Reagents and conditions: (a) $NH_2C(=NH)NH_2 \cdot H_2CO_3$, EtOH; (b) CH_3I, K_2CO_3, DMF; (c) $RB(OH)_2$, Cs_2CO_3, $PdCl_2(PPh_3)_2$.

Scheme 2. Synthesis of Dihydroisocytosines **13**, **16**[a]

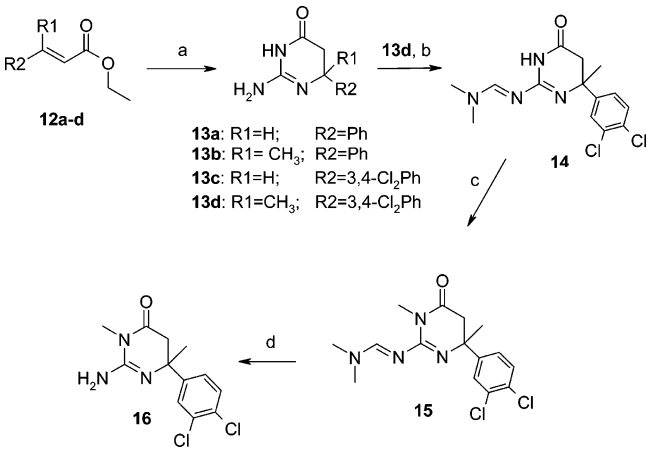

[a] Reagents and conditions: (a) $NH_2C(=NH)NH_2 \cdot HCl$, NaOMe, EtOH or NMP; (b) $(CH_3)_2NCH(OCH_3)_2$, DMF; (c) CH_3I, K_2CO_3, DMF; (d) 7N NH_3/MeOH.

N^3-methyl-substituted intermediate **21**. Deprotection of the N^1-methoxybenzyl group[46] afforded intermediate **22**. Hydrogenation to remove bromide of **22a** afforded the 6-phenyl analogue **23**. As with the isocytosines, Suzuki coupling of **22a**,**b** afforded the biphenyl analogues **24**−**27**. Separation of **27** into its enantiomers **28** and **29** was achieved by chiral SFC.

Assays. A key component of our fragment-based lead generation strategy was the utilization of X-ray crystal structures of fragments bound to BACE-1 to evolve the fragments to more potent compounds. Crystal structures of low affinity fragments are an invaluable aid for progressing them by allowing the determination of binding orientation, the degree of subsite occupancy, and polar interactions. However, these structures cannot quantitatively assess the functional relevance of any binding interactions; an enzyme inhibition assay is required to accomplish this. Without such a functional assay, it cannot be assured that any new binding interactions actually increase the affinity of the ligand for the enzyme. We used a fluorescence resonance energy transfer (FRET) assay as our standard assay for determination of functional inhibition. However, because of the observed propensity for nonspecific inhibition of BACE-1 at high ligand concentrations together with solubility limitations of many ligands under the FRET assay conditions, we found the FRET assay often to be unreliable for determining potencies >100 μM. To assist in the determination of the rank order potency of fragment hits (FRITs) with affinities between 1000 and 100 μM, we employed surface plasmon resonance (SPR) spectroscopy, a technique which allows determination of binding constants as well as identification of compounds with noncompetitive modes of inhibition. The third assay we utilized was an electrochemoluminescence-based assay and is referred to as the IGEN assay. This assay was used for compounds having intrinsic color or fluorescence that interfered with the FRET colorimetric readout. Because of the fact that the various assays were brought on stream at different times and that the use of a particular assay was dependent upon compound properties and potency ranges, only a limited number of compounds in this report have inhibition values reported for all three assays. However, as can be seen in Table 1, where a compound has inhibition data from all three assays, the agreement was quite good, with a difference of generally less than two-fold. Consequently, we were confident in assessing the relative potency between compounds even when the inhibition values were from different assays, especially since the goal during this phase of the project was not to identify structural changes that resulted in minor improvements in potency but rather to drive potency increases of low affinity FRITs to submicromolar potency and to identify preferred core scaffolds. Details of the assays are included in the Experimental Section.

Crystallography. A key component of our FRIT evolution strategy was the determination of the structures of our inhibitors bound to BACE-1. We previously described the method for the production of BACE-1 protein crystals suitable for soaking experiments.[47] Compounds were soaked into the BACE-1 crystals. AutoSolve was used to fit and score fragments into the Fo-Fc electron density maps that were calculated after initial automatic refinement against an unligated BACE-1 structure. Protein ligand structures of bound compounds were then subjected to further refinement steps. Table 2 lists the crystallographic data for the three structures reported herein.

Results and Discussion

We embarked on our search for drug-like BACE-1 inhibitors by implementing more traditional lead generation approaches such as high-throughput screening, rational design of pseudopeptidic transition-state isosteres, and virtual screening using the published crystal structure of BACE-1 complexed with OM99-2.[26] While we did identify pseudopeptidic inhibitors with potencies of <10 μM, they lacked defined SAR and we were unable to maintain this level of potency in compounds with good LE (>0.25). We encountered a different issue with hits derived from HTS and virtual screening. Utilizing NMR to assess the mechanism of inhibition, we discovered that many of the HTS and virtual screening hits were noncompetitive inhibitors, and thermal unfolding studies in the presence of those hits suggested that some of these owed their inhibition to destabilization of the BACE-1 tertiary structure. Consequently, we did not consider any of the hits from HTS or virtual screening sufficiently attractive and decided not to pursue them.

Scheme 3. Synthesis of Dihydroisocytosines **23**−**29**[a]

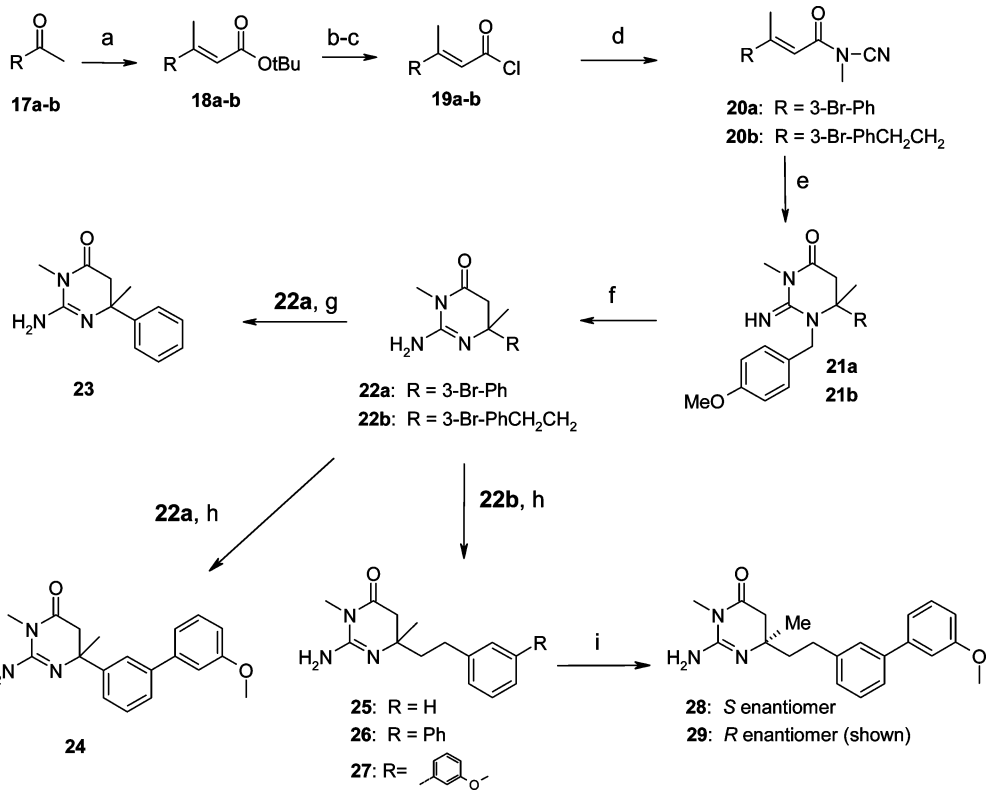

[a] Reagents and conditions: (a) $(CH_3O)_2P(O)CH_2CO_2tBu$, n-BuLi, THF; (b) 50% TFA/DCM; (c) oxalyl chloride, DMF (cat.), DCM; (d) *N*-methylcyanamide prepared from BrCN, NH_2CH_3, Na_2CO_3, THF; (e) 4-MeOBnNH$_2$, DMF; (f) $(NH_4)_2Ce(NO_3)_6$, acetonitrile, H_2O; (g) H_2, $Pd(OH)_2$, TEA, MeOH; (h) $RB(OH)_2$, $Pd(PPh_3)_2Cl_2$, K_3PO_4, DME, H_2O, EtOH, for **25** no $RB(OH)_2$; (i) chiral HPLC resolution.

Table 1. Activity Data for Isocytosines and Dihydroisocytosines[a]

compd	SPR % Inhib 1 mM	SPR % Inhib 500 μM	SPR IC_{50} (μM)	FRET IC_{50} (μM)	IGEN IC_{50} (μM)	cell assay IC_{50} (μM)	LE based on FRET
5	28						
6	62						
7	42						
8a	69						
8b	NV						
8c	89		86	130			0.28
8d	NT						
8e	NT						
8f		0					
10a		72	180	220	150		0.29
10b	69		28	36	27		0.29
10c	94		16	77	46		0.28
10d				29	30		0.27
11a			24		190		
11b	90		51	99	120		0.25
11c			5.7	5.9	5.3	91	0.29
13a		20					
13b		69	140	190			0.34
13c	42		480				
13d			79	82			0.33
16	93	60	7.5	6.1		3.5	0.39
23				2.0	3.8	3.8	0.49
24			0.67	0.38	0.28	0.59	0.36
25				34			0.34
26				1.6		1.7	0.33
27				0.20		0.64	0.35
28				35			0.23
29				0.08		0.47	0.37

[a] NV = no value obtained; NT = not tested.

The lack of success employing these traditional approaches led us to investigate fragment-based lead generation. As described in the accompanying article, we implemented 1D NMR screening of fragment libraries.[40] While a number of fragments were discovered that competitively inhibited BACE-1, the lead structure that emerged from this effort was the 6-propylisocytosine **5**. In the surface plasmon resonance (SPR) assay, compound **5** had an inhibition of 28% at 1 mM (Table 1). Screening of related structures from our corporate compound collection identified three additional isocytosines, **6**−**8a**. Com-

Table 2. Crystallographic Data Collection and Refinement Statistics

	8c	24	27
		Data Collection	
X-ray source	SRS 14.1, $\lambda = 0.977$ Å	ESRF ID14.2, $\lambda = 0.933$ Å	ESRF ID14.3, $\lambda = 0.931$ Å
resolution (Å)	2.75	2.5	2.2
no. unique reflections	13125	17850	25942
completeness (%)[a]	98.8(99.9)	99.9(100)	99.9(100)
average multiplicity	2.4	2.5	2.5
R_{merge}[a,b]	12.1(46)	6.9(39.6)	6.6(41.8)
		Refinement	
R_{cryst}	22.8	22.4	22.3
R_{free}	31.9	28.9	28.0
rmsd bond lengths (Å)	0.012	0.013	0.015
rmsd bond angles (deg)	1.4	1.5	1.5
average B-factor protein (Å^2)	45.7	47.5	41.5
average B-factor ligand (Å^2)	54.7	45.1	26.4
average B-factor solvent (Å^2)	30.0	37.7	40.1

[a] Numbers in parentheses indicate the highest shell values. [b] $R_{merge} = \Sigma_h\Sigma_i|I(h,i)-\langle I\rangle(h)|\Sigma hSi\langle I\rangle(h)$; $I(h,i)$ is the scaled intensity of the ith observation of reflection h, and $\langle I\rangle(h)$ is the mean value. Summation is over all measurements. $R_{cryst} = \Sigma_{hkl,work}||F_{obs}| - k|F_{calc}||/\Sigma hkl|F_{obs}I$, where F_{obs} and F_{calc} are the observed and calculated structure factors, k is a weighting factor and work denotes the working set of 95% of the reflections used in the refinement. $R_{free} = \Sigma_{hkl,test}||F_{obs}| - k|F_{calc}||/\Sigma_{hkl}|F_{obs}|$, where F_{obs} and F_{calc} are the observed and calculated structure factors, k is a weighting factor, and test denotes the test set of 5% of the reflections used in cross validation of the refinement. λ refers to wavelength, R_{msd} to root-mean-square deviations.

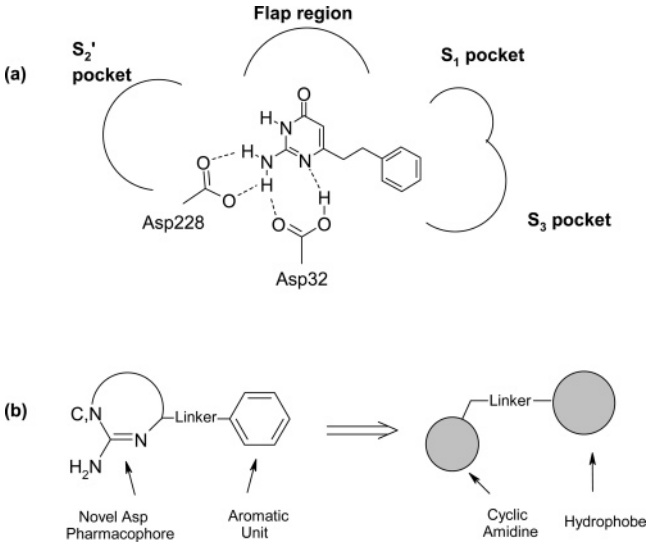

Figure 2. (a) Interactions of isocytosine with endothiapepsin. (b) Novel cyclic amidine-based aspartyl protease pharmacophore.

pound **8a** was the most potent, with an inhibition at 1 mM of 69% in the SPR assay. We were able to determine the binding mode of **8a** from the X-ray structure of its complex with endothiapepsin.[40] We used endothiapepsin as a surrogate for BACE-1 since at the time we initiated these studies we did not have access to suitable crystals of BACE-1. The interactions of the isocytosine core with the catalytic aspartates are illustrated in Figure 2a.

Ultimately, a collaboration was established with Astex Therapeutics who had successfully crystallized apo-BACE-1 in a crystal form that allowed for fragment soaking. Astex had independently identified a class of 2-aminopyridine BACE-1 inhibitors via their high throughput crystallography technology.[38] While the aminopyridines and isocytosines are distinct scaffolds with differing physicochemical properties, they shared two important enzyme recognition features: a cyclic amidine motif that interacts with the catalytic aspartates, and a hydrophobic substituent in the 6-position that binds in the S_1 subsite of BACE-1. It was quickly recognized that these binding elements represented a novel, nonpeptidic aspartyl protease pharmacophore, depicted in Figure 2b, and we therefore focused our efforts on exploiting this novel finding. Optimization of the aminopyridine series has been previously described.[39]

Our initial efforts with the isocytosine series focused on improving potency by optimizing the 6-subsituent for binding in the S_1/S_3 subsites, which form a contiguous, relatively hydrophobic binding pocket. Lengthening or shorting of the 6-position linker reduced activity relative to the two-carbon ethyl group **8a** (**7, 8f**). Consequently, the rest of our studies in the isocytosine series used the ethyl linker. The napthyl analogue **8b** was prepared to more fully fill the S_1/S_3 subpockets. However, we were not able to generate an IC_{50} value because of the compound's poor solubility. To increase solubility, and potentially exploit a hydrogen bond interaction with the enzyme, the indole derivative **8c** was prepared, which had an SPR IC_{50} of 86 μM, and 130 μM in the FRET assay. The crystal structure of BACE-1 complexed with **8c** indicated that a hydrogen bond was formed between the indole NH and the carbonyl oxygen atom of Gly-230 (Figure 3). The N^1 nitrogen atom and exocyclic NH_2 group of the isocytosine core forms hydrogen bonds with the catalytic aspartates as anticipated from the structures of the aminopyridines in BACE-1[38,39] and of **8a** in endothiapepsin.[40]

An additional observation from the structure of **8c** complexed with BACE-1 was that the N^3 NH group does not form any interactions with the enzyme and is pointed toward the S_2' subsite. This finding led us to investigate substitutions on the N^3 nitrogen atom. We found that a simple methyl substituent modestly increased potency. Thus, the *N*-methyl phenethyl analogue **10a** had a FRET IC_{50} of 220 μM while the IC_{50} was 77 μM for the N^3 methylated indolyl analogue **10c** (vs 130 μM for **8c**). N-Methylation also allowed determination of an IC_{50} for the 6-napthethyl-substituted isocytosine **10b**. With an SPR IC_{50} of 28 μM, and 36 μM in the FRET assay, **10b** was the most potent isocytosine identified at this point.

Examination of the BACE-1 crystal structures of **8c** (Figure 3) and the aminopyridines[39] suggested that the bicyclic substituents were not fully occupying the S_1/S_3 subsite. This led us to incorporate biphenyl-based substituents (**10d, 11a**−**c,** Table 1). Because of intrinsic fluorescence, the IC_{50} of **11a** could not be determined in the FRET assay. Compound **11c**, with IC_{50} values of 5.7, 5.9, 5.3 μM (SPR, FRET, IGEN assays, respectively), was the most potent isocytosine identified.

As part of our exploration of the isocytosine series, we screened related 2-amino heterocycles from our corporate compound collection. The most promising hit we identified was the dihydroisocytosine **13a**, which had an SPR inhibition of 20%

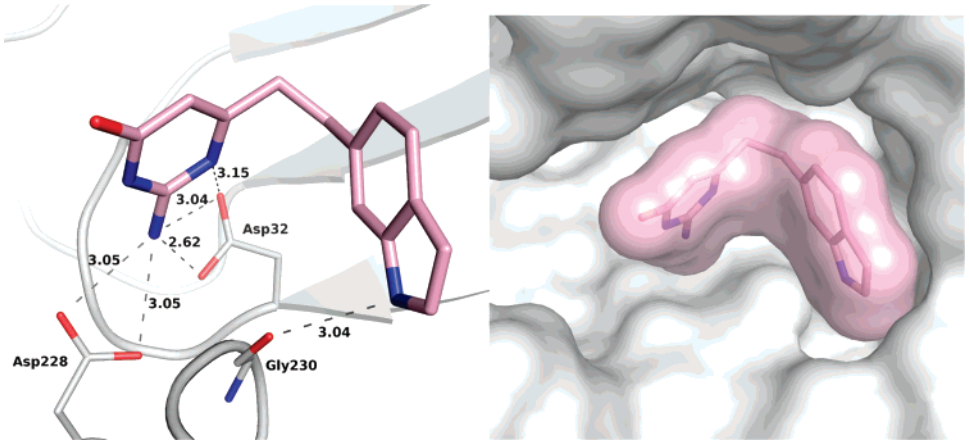

Figure 3. Structure of **8c** complexed with BACE-1. All pictures in this section were generated using PyMOL Molecular Graphics System: DeLano, W.L. *The PyMOL Molecular Graphics System*; DeLano Scientific: Palo Alto, CA.

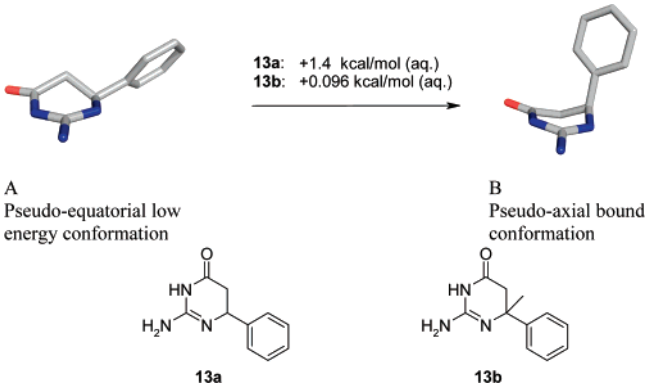

Figure 4. Energy difference between the pseudoequatorial conformation of **13a** (A) and the bound pseudoaxial conformation (B), and the energy difference between the conformations of the 6-methyl analogue **13b**. Initial conformations were generated in an MMFF conformational search. AM1 geometry optimization of the lowest energy pseudoaxial and pseudoequatorial conformations preceded HF/6−316* energy calculations. Aqueous solvation energies are from the SM5.4 model. All calculations were performed in Spartan '02.

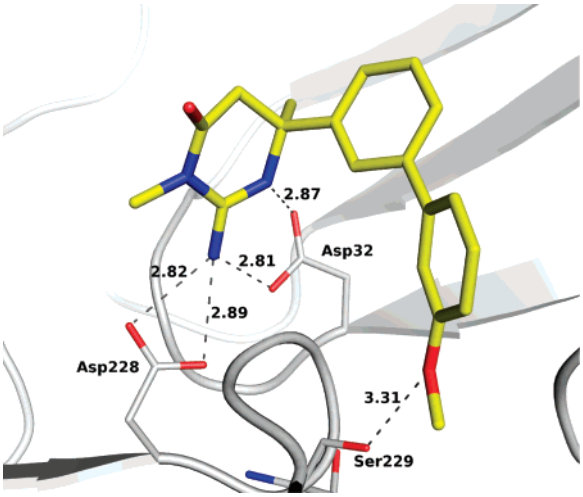

Figure 5. Structure of **24** complexed with BACE-1.

at 500 μM (Table 1). Incorporation of a 6-dichlorophenyl group increased potency, with **13c** having an SPR IC_{50} of 480 μM. While a crystal structure of **13a** was obtained, the resolution of the structure was low. However, the resolution was sufficient to reveal that the bound conformation of **13a** had the 6-phenyl group oriented in the less favorable pseudoaxial conformation (Figure 4). Calculations indicated that the psuedo-axial conformation was 1.4 kcal higher in energy than the pseudoequatorial conformation in water (1.7 kcal/mol in gas phase). This led us to incorporate a 6-methyl substituent in an attempt to increase the relative stability of the pseudoaxial conformation, thus reducing the energetic penalty for adoption of the higher energy pseudoaxial bound conformation and thereby increase potency. The calculated energy difference between the pseudoaxial and pseudoequatorial conformations is less than 0.1 kcal/mol for the 6-methyl analogue in water and slightly favored in the gas phase (−0.53 kcal/mol). We were also concerned about possible metabolic oxidation of the 6-H dihydroisocytosine to the corresponding isocytosine, a process that would be blocked by the 6-methyl substituent. Incorporation of a 6-methyl group into **13a** afforded **13b**, which had IC_{50} values of 140 μM (SPR) and 190 μM (FRET), while the 6-methyl dichlorophenyl analogue **13d** had an IC_{50} of 82 μM (FRET).

As anticipated from the SAR of the isocytosines, an N^3-methyl group further increased potency. The 3-methyl-6-dichlorophenyl dihydroisocytosine **16** and the 3-methyl-6-phenyl dihydroisocytosine **23** both had single digit micromolar potency and demonstrated a >10-fold increase in activity relative to their nonmethylated congeners. In addition, each demonstrated functional cellular activity with IC_{50} values of approximately 4 μM (Table 1). Incorporation of the biphenyl methoxy motif afforded **24**, which with a FRET IC_{50} of 380 nM and an IC_{50} of 590 nM in the cell-based assay was the first submicromolar BACE-1 inhibitor we identified. Thus, by leveraging the knowledge gained from the aminopyridine and isocytosine structure−activity studies, we were able to rapidly progress the dihydroisocytosines through targeted synthesis of only seven compounds to sub-micromolar potency. The ligand efficiency of the dihydroisocytosines was significantly better than that of the isocytosines, as was their potency and solubility. As a result, the dihydroisocytosines emerged as our leading series.

Examination of the crystal structure of **24** revealed that the oxygen atom of the 3′-methoxy substituent displaced a water molecule present in the apo-BACE-1 structure and formed a hydrogen bond with the hydroxyl group of Ser-229 (Figure 5). In addition, it appeared that the phenyl group directly attached to the dihydroisocytosine core did not optimally fill the S_1 pocket when compared to the ethyl-linked phenyl group in the isocytosines such as **11** (Figure 3). It was not clear that use of an ethyl linker would improve the potency of the dihydroisocytosines because of the penalty from increasing rotational entropy that this modification would introduce. To investigate the phenethyl linker in the dihydroisocytosines, we prepared compounds **25**−

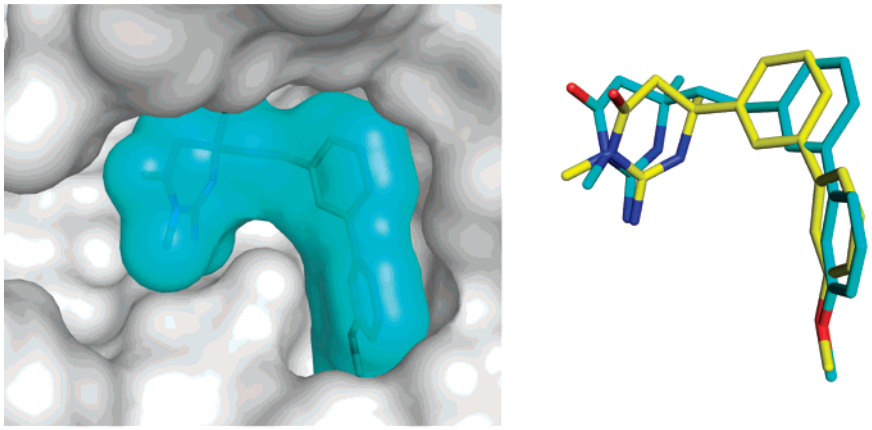

Figure 6. (a) Structure of **27** complexed with BACE-1. (b) The overlap of **24** (yellow) with **27** (cyan).

27. While compound **25** was less potent than the corresponding phenyl-linked analogue **23**, the biphenyl methoxy analogue **27** was slightly more potent than **24**. Compound **27** was also active in the cell-based assay with an IC_{50} of 640 nM. The structure of the complex of **27** with BACE-1 illustrates how well **27** fills the S_1/S_3 subsites (Figure 6a). The overlap of the bound structures of **27** and **24** reveals that the biphenyl group of **27** extends a little deeper into the S_1/S_3 subsite, and that the dihydroisocytosine core is tilted toward the S′ subsites while maintaining the key interactions with the catalytic aspartates and Ser-229.

Chromatographic separation of the enantiomers of **27** afforded the two pure enantiomers, **28** and **29**. The absolute stereochemical assignment was based on the activity of the compounds and analogy with the stereochemistry of the bound conformation in the crystal structure of **27**. Thus, the inactive isomer, **28**, was assigned the *S* configuration, while the active isomer, **29**, was assigned the *R* configuration. With a FRET IC_{50} of 80 nM, **29** was the most potent compound we have identified to date, was active in the cell-based assay, and possessed very high ligand efficiency (0.37).

Conclusion

Using NMR screening, we identified a novel series of cyclic amidines with millimolar potency. The application of several different biophysical methodologies allowed evolution of these weak fragment hits to micromolar inhibitors of BACE-1. Screening of related structures resulted in the discovery of the dihydroisocytosines, a series that afforded compounds with high potency and cellular activity. Translation of SAR from the isocytosines allowed us to rapidly and efficiently increase potency in the dihydroisocytosine series. Ligand efficiency was used to guide the optimization of inhibitor series and assess the intrinsic binding avidity of core structures. The cyclic amidine motif represents a novel aspartyl protease core and should find application to the design and development of inhibitors of other aspartyl proteases such as renin and HIV protease. Future publications from our group will detail the evolution of this pharmacophore to new core structures with greater intrinsic potency.

Experimental Section

Chemistry. Proton magnetic resonance (^{1}H NMR) spectra were recorded on a Bruker Avance DPX 300 MHz spectrometer, and the chemical shifts are reported in parts-per-million (δ) from a tetramethylsilane internal standard. High-resolution mass spectra were recorded on an Agilent Technologies 6210 Time-of-Flight LC/MS spectrometer. The heating of reactions with microwaves was performed on a Personal Chemistry Smith Synthesizer unit (monomodal, 2.45 GHz, 300 W max.) for the times indicated. Analytical supercritical fluid chromatography (SFC) was performed on a Berger Instruments SFC Analytix Platform and preparative SFC chromatography performed on the Berger Multigram II Preparative-SFC. Standard silica gel flash chromatography was employed as a method for purification of intermediates with the indicated solvent mixtures. Alternately, intermediates were also purified on an Isco CombiFlash Sq 16x instrument using prepackaged disposable RediSep SiO_2 stationary phase columns (4, 12, 40, 120 g sizes) with gradient elution at 5−125 mL/min of selected bisolvent mixture, UV detection (190−760 nm range) or timed collection, 0.1 mm flow cell path length.

All solvents and reagents were obtained from commercial sources and used without further purification unless otherwise noted. Compounds **5**−**7** were obtained from the AstraZeneca corporate compound collection as was the initial screening sample for **8a**. Compound **8a** was resynthesized for conformation of structure, purity, and activity as described below. HPLC purification conditions can be found in the Supporting Information.

2-Amino-6-phenethyl-3*H*-pyrimidin-4-one (8a). To a solution of **9a** (2.36 g, 10.7 mmol) in ethanol (36 mL) was added guanidine carbonate (0.97 g, 5.4 mmol), and the reaction was heated under reflux overnight. The reaction was allowed to cool, and the resulting solid was collected by filtration and rinsed with ethanol (10 mL). The solid was dried under reduced pressure to give the desired product as a white solid (1.47 g, 64%). ^{1}H NMR (300 MHz, DMSO-d_6) δ 2.53 (t, J = 9.4 Hz, 2H), 2.85 (t, J = 7.9 Hz, 2H), 5.39 (s, 1H), 6.46 (s, 2H), 7.30 (m, 5H), 10.57 (s, 1H); MS (ES+) m/z 216 $[M + H]^+$; HRMS (TOF) m/z calcd for $C_{12}H_{13}N_3O$ $[M + H]^+$, 216.1131; found, 216.1137.

2-Amino-6-[2-(1*H*-indol-6-yl)ethyl]pyrimidin-4(3*H*)-one (8c). To **9c** (approximately 65% pure with over-reduced product as the major contaminant) (20 g, 77 mmol) was added ethanol (160 mL) under argon, and to this was added guanidine carbonate (9.0 g, 50 mmol). The reaction was heated under reflux overnight and then concentrated until approximately 50 mL of ethanol remained. To this was added water (50 mL), and the mixture was stirred for 3 h. The resulting solid was collected by filtration, washed with water (approximately 50 mL), and then dried under reduced pressure at 60 °C overnight to give the title compound as a yellow solid (7.9 g, 62%). Another batch of the title compound slowly crystallized from the filtrate to afford a white solid (2.4 g, 19%). ^{1}H NMR (300 MHz, DMSO-d_6) δ 2.56 (t, J = 7.9 Hz, 2H), 2.93 (t, J = 7.9 Hz, 2H), 5.36 (s, 1H), 6.34 (d, J = 2.9 Hz, 1H), 6.62 (s, 2H), 6.85 (d, J = 8.0 Hz, 1H), 7.18 (s, 1H), 7.23 (d, J = 3.1 Hz, 1H), 7.41 (d, J = 8.1 Hz, 1H), 10.90 (s, 1H); MS (APCI+) m/z 255 $[M + H]^+$; HRMS (TOF) m/z calcd for $C_{14}H_{14}N_4O$ $[M + H]^+$, 255.1240; found, 255.1241.

2-Amino-6-[2-(3-bromophenyl)ethyl]pyrimidin-4(3*H*)-one (8e). To a solution of **9e** (9.72 g, 32 mmol) in ethanol (120 mL) was added guanidine carbonate (2.9 g, 16 mmol), and the reaction was heated under reflux overnight. The reaction was allowed to cool and the resulting solid collected by filtration and washed with ethanol (20 mL). The solid was dried under reduced pressure to give the title compound as a white solid (6.8 g, 71%). ^{1}H NMR (300 MHz, DMSO-d_6) δ 2.53 (t, $J = 8.1$ Hz, 2H), 2.86 (t, $J = 7.8$ Hz, 2H), 5.39 (s, 1H), 6.46 (s, 2H), 7.23 (m, 2H), 7.37 (m, 1H), 7.42 (s, 1H), 10.58 (s, 1H); MS (APCI+) *m*/*z* 294 $[M + H]^+$.

Ethyl 5-(2-Naphthyl)-3-oxopentanoate (9b). Diisopropylamine (8.7 mL, 62 mmol) was dissolved in THF (100 mL) under nitrogen and cooled to 0 °C, and to this was added *N*-butyllithium (1.6 M, 3.8 mL, 65 mmol). The resulting solution was then added to ethyl acetoacetate (3.8 mL, 30 mmol) and allowed to stir at 0 °C for approximately 25 min. Next, a solution of 2-(bromomethyl)-naphthalene (6.6 g, 30 mmol) in THF (90 mL) was added over approximately 45 min. The reaction was allowed to stir for 3 h at 0 °C and then quenched with a mixture of concentrated HCl (5.2 mL), water (14 mL), and diethyl ether (40 mL). The mixture was stirred for 20 min and then partitioned between diethyl ether (300 mL) and water (150 mL). The layers were separated, and the aqueous phase was extracted with diethyl ether (150 mL). The combined organics were washed approximately 10 times with water (10 × 100 mL), dried over sodium sulfate, and concentrated under reduced pressure. The resulting material was purified by silica gel chromatography using hexanes/DCM (8:2, 1:1, 2:8) step gradient to give the title compound as a light yellow liquid (2.83 g, 36%). ^{1}H NMR (300 MHz, $CDCl_3$) δ 1.24 (t, $J = 7.1$ Hz, 3H), 2.97 (m, 2H), 3.08 (m, 2H), 3.43 (s, 2H), 4.17 (q, $J = 7.1$ Hz, 2H), 7.31 (m, 1H), 7.44 (m, 2H), 7.62 (s, 1H), 7.78 (m, 3H); MS (APCI+) *m*/*z* 293 $[M + Na]^+$.

Ethyl 5-(1*H*-Indol-6-yl)-3-oxopentanoate (9c). 6-Formylindole (15.0 g, 103 mmol) was dissolved in dry THF (410 mL) under argon, to this was added [3-(ethoxycarbonyl)-2-oxopropyl]triphenylphosphonium chloride (66.0 g, 155 mmol), and the reaction was cooled to 5 °C. Sodium hydride (60%, 6.50 g, 412 mmol) was then added in portions over 10 min, the cooling bath removed, and the reaction allowed to stir overnight. Another portion of sodium hydride (60%, 4.10 g, 102 mmol) was added, the reaction allowed to stir for 2 h, and then another portion of [3-(ethoxycarbonyl)-2-oxopropyl]triphenylphosphonium chloride (22 g, 51 mmol) added. The reaction was again allowed to stir overnight and cooled to 5 °C, and to this were added saturated aqueous ammonium chloride (200 mL) and water (100 mL). Ethyl acetate (100 mL) was added and the product extracted into the organic phase. The organic phase was dried over sodium sulfate, filtered, concentrated under reduced pressure, and purified by silica gel chromatography (30% ethyl acetate/hexanes) to give ethyl (4*E*)-5-(1*H*-indol-6-yl)-3-oxopent-4-enoate[48] as a white solid (20.6 g, 78%). ^{1}H NMR (300 MHz, DMSO-d_6) δ 1.20 (t, $J = 7.1$ Hz, 3H), 3.85 (s, 2H), 4.12 (q, $J = 7.1$ Hz, 2H), 6.49 (s, 1H), 6.83 (d, $J = 16.1$ Hz, 1H), 7.39 (d, $J = 8.3$ Hz, 1H), 7.49 (m, 1H), 7.59 (d, $J = 8.3$ Hz, 1H), 7.72 (s, 1H), 7.79 (d, $J = 16.1$ Hz, 1H), 11.38 (s, 1H); MS (ES−) *m*/*z* 256 $[M - H]^-$.

Ethyl (4*E*)-5-(1*H*-indol-6-yl)-3-oxopent-4-enoate (20.6 g, 80 mmol) was dissolved in ethanol (160 mL) under argon, the solvent was degassed with argon, and 10% Pd/C (4.25 g) was added. The mixture was placed under 1 atm of hydrogen and stirred vigorously for 2 h. The mixture was filtered through Celite, washed with ethanol, and concentrated under reduced pressure to give (20 g, 77 mmol) of a white solid consisting of a 65:35 mixture of product and over-reduced material which was used without further purification. MS (ES−) *m*/*z* 258 $[M - H]^-$.

Ethyl 5-(3-Bromophenyl)-3-oxopentanoate (9e). To a round-bottom flask was added magnesium chloride (10.4 g, 109 mmol), acetonitrile (580 mL), potassium malonate (15.6 g, 92.0 mmol), and TEA (19.5 mL, 140 mmol). Separately, 3-(3-bromophenyl)-propionic acid (10 g, 44 mmol) was dissolved in acetonitrile (200 mL), and to this was added 1,1′-carbonyldiimidazole (CDI) (7.8 g, 48 mmol). Both were allowed to stir for approximately 2.5 h, and then the 3-(3-bromophenyl)propionic acid/CDI solution was added dropwise to the mixture of $MgCl_2$, potassium ethyl malonate, and TEA. The reaction was stirred overnight and then heated at 90 °C for 3 h. It was then allowed to cool to room temperature, filtered, and rinsed with acetonitrile (3 × 100 mL). The combined filtrates were concentrated under reduced pressure and then partitioned between methylene chloride and water. The product was extracted into the methylene chloride layer, washed with 10% aqueous citric acid solution, dried over sodium sulfate, filtered, and concentrated under reduced pressure to give the title compound which was used without purification (9.72 g, 75%). MS (APCI+) *m*/*z* 299 $[M + H]^+$.

2-Amino-3-methyl-6-phenethyl-3*H*-pyrimidin-4-one (10a). To a stirred solution of **8a** (410 mg, 1.89 mmol) in DMF (36 mL) were added potassium carbonate (260 mg, 1.89 mmol) and iodomethane (0.12 mL, 1.89 mmol). The reaction was allowed to stir for 3 days and then added to a large volume of water. The material was extracted into diethyl ether (2 × 60 mL), dried over sodium sulfate, filtered, and concentrated under reduced pressure. Because of residual DMF, additional water was added with the resulting white solid collected by filtration and dried overnight under reduced pressure to give the title compound as a white solid (82 mg, 19%). ^{1}H NMR (300 MHz, DMSO-d_6) δ 2.53 (t, $J = 9.9$ Hz, 8H), 2.86 (t, $J = 8.0$ Hz, 5H), 3.21 (s, 6H), 5.50 (s, 2H), 7.05 (s, 3H), 7.22 (m, 9H); MS (APCI+) *m*/*z* 230 $[M + H]^+$; HRMS (TOF) *m*/*z* calcd for $C_{13}H_{15}N_3O$ $[M + H]^+$, 230.1288; found, 230.1292.

2-Amino-6-[2-(3-bromophenyl)ethyl]-3-methylpyrimidin-4(3*H*)-one (10e). To a stirred solution of **8e** (6.7 g, 23 mmol) in DMF (410 mL) were added potassium carbonate (2.8 g, 20 mmol) and iodomethane (1.3 mL, 20 mmol). The reaction was allowed to stir for 3 days, and then another portion of potassium carbonate (0.94 g, 7 mmol) and iodomethane (0.43 mL, 7 mmol) was added. The reaction was again allowed to stir overnight and then added to a large volume of water (approximately 8 L). The material was extracted into diethyl ether (6 × 200 mL), and the resulting solution was concentrated under reduced pressure. A portion of the resulting solid (3.0 g) was stirred in methylene chloride (260 mL) and then filtered to give the desired product as a white solid (2.2 g, 92%). ^{1}H NMR (300 MHz, DMSO-d_6): δ 2.54 (t, 2H, $J = 8.5$ Hz), 2.87 (t, 2H, $J = 7.7$ Hz), 3.22 (s, 3H), 5.50 (s, 1H), 7.07 (s, 2H), 7.24 (m, 2H), 7.37 (m, 1H), 7.43 (s, 1H); MS (APCI+) *m*/*z* 308 $[M + H]^+$; HRMS (TOF) *m*/*z* calcd for $C_{13}H_{14}BrN_3O$ $[M + H]^+$, 308.0398; found, 308.0348.

2-Amino-3-methyl-6-[2-(3-pyridin-3-ylphenyl)ethyl]-3*H*-pyrimidin-4-one (11a). To **10e** (TFA salt) (0.050 g, 0.12 mmol) was added a solution of dimethoxyethane/water/ethanol (7:3:2 ratio, 2 mL) followed by pyridine-3-boronic acid (0.020 g, 0.16 mmol), cesium carbonate (0.12 g, 0.36 mmol), and dichlorobis(triphenylphosohine)palladium(II) (5 mg, 0.006 mmol), and the mixture was heated by microwave at 150 °C for 15 min. Insoluble materials were removed by filtration, and the solution was purified by Method E to afford the desired product as a white TFA salt (80 mg, 40%). ^{1}H NMR (300 MHz, DMSO-d_6) δ 2.80 (t, $J = 7.7$ Hz, 2H), 2.99 (t, $J = 7.7$ Hz, 2H), 3.26 (s, 3H), 5.86 (s, 1H), 7.36 (d, $J = 7.6$ Hz, 1H), 7.47 (t, $J = 7.6$ Hz, 1H), 7.73−7.59 (m, 3H), 8.30 (d, $J = 8.0$ Hz, 1H), 8.72−8.63 (m, 3H), 8.99 (s, 1H); MS (APCI+) *m*/*z* 307 $[M + H]^+$; HRMS (TOF) *m*/*z* calcd for $C_{18}H_{18}N_4O[M + H]^+$, 307.1559; found, 307.1598.

3-(3,4-Dichlorophenyl)but-2-enoic Acid Ethyl Ester (12d). To a −78 °C stirred solution of triethyl phosphonoacetate (11.5 mL, 58.2 mmol) in THF (100 mL) was added n-BuLi in hexanes (1.6 N, 38 mL, 61 mmol), and the reaction was stirred at −78 °C for 10 min. To this mixture was added a solution of 3,4-dichloroacetophenone (10.0 g, 52.9 mmol) in THF (10 mL), and the reaction was allowed to warm to room temperature and stirred for 18 h. The solvent was removed under reduced pressure to yield a yellow solid. To this was added 400 mL 1:3 Et_2O: hexanes, and the solids were triturated for 1 h. The resulting precipitate was removed by filtering through Celite, and the filtrate was collected and concentrated under reduced pressure to give the title compound as a crude orange oil (12.14 g, 88%). This material was carried directly into

the next reaction without further purification. ^{1}H NMR (300 MHz, DMSO-d_6) δ 1.24 (t, J = 6.9 Hz, 3H), 2.48 (s, 3H), 6.22 (s, 1H), 7.50 (d, J = 2.4 Hz, 1H), 7.84 (d, J = 2.1 Hz, 2H).

2-Amino-6-(3,4-dichlorophenyl)-6-methyl-5,6-dihydro-3*H*-pyrimidin-4-one (13d). To a solution of **12d** (100 mg, 0.386 mmol) in 2.0 mL of NMP were added guanidine hydrochloride (147 mg, 1.54 mmol) and sodium methoxide (62.0 mg, 1.62 mmol), and the reaction was subjected to microwaves at 200 °C for 10 min. The solids were filtered from the reaction, and the filtrate was used directly for purification using Method C. The combined purified fractions were lyophilized to give the title compound as a white TFA salt (49 mg, 33%). ^{1}H NMR (300 MHz, DMSO-d_6–/TFA-d) δ 1.65 (s, 3H), 3.17 (m, 1H), 3.36 (d, J = 16.5 Hz, 1H), 7.42 (d, J = 8.4 Hz, 1H), 7.70 (m, 2H); MS (+ES) m/z 272 $[M + H]^+$; HRMS (TOF) m/z calcd for $C_{11}H_{11}Cl_2N_3O$ $[M + H]^+$, 272.0352; found, 272.0354.

***N*′-[4-(3,4-Dichlorophenyl)-4-methyl-6-oxo-1,4,5,6-tetrahydropyrimidin-2-yl]-*N*,*N*-dimethylformamidine (14).** To a stirred solution of **13d** (0.25 g, 0.94 mmol) in DMF (5 mL) was added dimethylformamide dimethylacetal (0.160 mL, 1.17 mmol), and the reaction was stirred for 2 h. The DMF was removed under reduced pressure to yield a pale yellow oil. The oil was purified by ether trituration (2 × 20 mL) to give the title compound as a colorless oil (0.30 g, 99%). ^{1}H NMR (300 MHz, DMSO-d_6) δ 1.67 (s, 3H), 3.11−3.17 (br s, 4H), 3.20−3.29 (br s, 4H), 7.47 (d, J = 8.4 Hz, 1H), 7.69 (d, J = 8.4 Hz, 1H), 7.76 (s, 1H), 8.56 (s, 1H); MS (ES +) m/z 327 $[M + H]^+$.

N′-[4-(3,4-Dichlorophenyl)-1,4-dimethyl-6-oxo-1,4,5,6-tetrahydropyrimidin-2-yl]-*N*,*N*-dimethylformamidine (15). To a stirred solution of **14** (0.31 g, 0.94 mmol) and potassium carbonate (0.140 g, 1.03 mmol) in DMF (70 mL) was added iodomethane (0.060 mL, 1.0 mmol), and the reaction was stirred for 18 h. To this mixture were added additional potassium carbonate (0.140 g, 1.03 mmol) and iodomethane (0.060 mL, 1.0 mmol), and the mixture was stirred an additional 18 h. The THF was removed under reduced pressure to yield a cloudy yellow oil. To this was added hexanes (250 mL), and the reaction was stirred for 10 min. The resulting precipitate was filtered and the filtrate concentrated under reduced pressure. The crude compound was purified using flash chromatography (silica gel, 5:95 ethyl acetate: hexanes) to give the title compound as a colorless oil (160 mg, 50%). ^{1}H NMR (300 MHz, DMSO-d_6) δ 1.67 (s, 3H), 3.11 (s, 3H), 3.19 (s, 3H), 3.22 (d, J = 16.5 Hz, 1H), 3.36 (s, 3H), 3.57 (d, J = 16.5 Hz, 1H), 7.49 (d, J = 8.3 Hz, 1H), 7.65 (d, J = 8.4 Hz, 1H), 7.82 (s, 1H), 8.65 (s, 1H); MS (ES +) m/z 341 $[M + H]^+$.

2-Amino-6-(3,4-dichlorophenyl)-3,6-dimethyl-5,6-dihydro-3*H*-pyrimidin-4-one (16). To a solution of **15** (0.16 g, 0.47 mmol) in MeOH (15 mL) was added 7 N methanolic ammonia (3.0 mL, 21 mmol), and the reaction was heated to 60 °C for 3 h. The MeOH was removed under reduced pressure to yield an amber syrup. To this was added acetonitrile:water:TFA (75:25:0.1, 4 mL), and the resulting mixture was filtered. The filtrate was purified using Method C. The combined purified fractions were lyophilized to give the title compound as a white TFA salt (30 mg, 22%). ^{1}H NMR (300 MHz, DMSO-d_6) δ 1.65 (s, 3H), 3.12 (s, 3H), 3.19 (d, J = 16.5 Hz, 1H), 3.50 (d, J = 16.5 Hz, 1H), 7.41 (d, J = 8.4 Hz, 1H), 7.67 (d, J = 8.4 Hz, 1H), 7.72 (s, 1H), 8.80 (br s, 2H), 10.46 (br s, 1H); MS (ES+) m/z 286 $[M + H]^+$; HRMS (TOF) m/z calcd for $C_{12}H_{13}Cl_2N_3O[M + H]^+$, 286.0508; found, 286.0515.

4-(3-Bromophenyl)butan-2-one (17b).[49] To 2,4-pentanedione (15.8 mL, 0.154 mol) in ethanol (150 mL) was added potassium carbonate (19.4 g, 0.140 mol) followed by 3-bromobenzyl bromide (35.0 g, 0.140 mol). The reaction was refluxed for 18 h and was cooled to room temperature, and the salts were removed by filtration. The filtrate was concentrated under reduced pressure and the resulting yellow solid partitioned between ethyl acetate and water (200 mL/100 mL). The ethyl acetate layer was washed twice with aqueous HCl (1 N, 100 mL), once with saturated aqueous sodium bicarbonate (100 mL), and once with saturated aqueous sodium chloride (100 mL), dried over sodium sulfate, and filtered, and the filtrate concentrated under reduced pressure. The resulting yellow oil was purified on silica gel (0.5 kg) in a large filter funnel eluting with 1 L each of a 5% step gradient 0−100% hexanes/methylene chloride to afford the title compound as a clear oil (18.5 g, 58%). ^{1}H NMR (300 MHz, DMSO-d_6) δ 2.10 (s, 3H), 2.79 (s, 4H), 7.22−7.24 (m, 2H), 7.35−7.39 (m, 1H), 7.43 (s, 1H).

3-(3-Bromophenyl)but-2-enoic Acid *tert*-Butyl Ester (18a). To a −78 °C stirred solution of *tert*-butyldimethyl phosphonoacetate (21.9 mL, 0.111 mol) in THF (150 mL) was added n-BuLi in hexanes (1.6 M, 72 mL, 0.12 mol), and the reaction was stirred at −78 °C for 10 min. To this mixture were added **17a** and 3′-bromoacetophenone (Aldrich) (13.4 mL, 0.100 mol), and the reaction was allowed to warm to room temperature and was stirred for 18 h. The THF was removed under reduced pressure to yield a yellow solid. To this was added hexanes (300 mL), and the solids were triturated for 1 h. The mixture was filtered through Celite and the filtrate concentrated under reduced pressure to give the title compound as a yellow oil (28.9 g, 97%). This was carried directly into the next reaction. ^{1}H NMR (300 MHz, DMSO-d_6) δ 1.20 (s, 3H), 1.47 (s, 6H), 2.10 (d, J = 1.4 Hz, 0.7H), 2.44 (d, J = 1.3 Hz, 1.3H), 5.87 (d, J = 1.5 Hz, 0.3H), 6.05 (d, J = 1.3 Hz, 0.7H), 7.19−7.38 (m, 2H), 7.49−7.59 (m, 2H), 7.71 (t, J = 1.8 Hz, 1H).

5-(3-Bromophenyl)-3-methylpent-2-enoic Acid *tert*-Butyl Ester (18b). To a −78 °C stirred solution of *tert*-butyldimethyl phosphonoacetate (19.5 mL, 89.61 mmol) in tetrahydrofuran (100 mL) was added n-butyllithium in hexanes (1.6 M, 35.8 mL, 89.61 mmol), and the reaction was stirred at −78 °C for 25 min. To this mixture was added **17b** (18.5 g, 81.5 mmol), the reaction was allowed to warm to room temperature and stirred for 1.5 h, and the solvent removed under reduced pressure. The resulting solid was triturated with hexanes (300 mL) for 1 h and filtered through Celite and the filtrate concentrated under reduced pressure to give a single isomer of the title compound as a clear oil that was used in the next reaction without further purification. ^{1}H NMR (300 MHz, DMSO-d_6) δ 1.42 (d, J = 3.2 Hz, 9H), 1.86 (d, J = 1.3 Hz, 1H), 2.12 (d, J = 1.1 Hz, 2H), 2.37−2.43 (m, 2H), 2.73−2.78 (m, 2H), 5.58−5.60 (m, 1H), 7.24 (d, J = 5.2 Hz, 2H), 7.35−7.40 (m, 1H), 7.45 (d, J = 5.4 Hz, 1H).

3-(3-Bromophenyl)but-2-enoyl Chloride (19a). A solution of **18a** (28.9 g, 0.097 mol) in trifluroracetic acid:methylene chloride (1:1, 300 mL) was stirred at room temperature for 15 min, and the solvents were removed under reduced pressure. The crude yellow solid was triturated in hexanes (400 mL), filtered, and dried under reduced pressure to afford a single isomer of 3-(3-bromophenyl)-but-2-enoic acid as a white solid (8.87 g, 38%). ^{1}H NMR (300 MHz, DMSO-d_6) δ 2.46 (s, 3H); 6.11 (s, 1H); 7.37 (t, J = 7.8 Hz, 1H); 7.53 (m, 2H); 7.72 (t, J = 1.5 Hz, 1H). The filtrate was removed of solvent under reduced pressure, resulting in a second impure batch of mixed isomers, which was dried under high vacuum over night (15 g). The dry material was triturated with hexanes (500 mL, 0.12 M) at room temperature for 30 min. The precipitate was filtered to give a very pale yellow solid consisting of mixed isomers (10.2 g, 44%). ^{1}H NMR (300 MHz, DMSO-d_6/TFA-d) δ 2.13 (s, 0.6H), 2.49 (s, 0.4), 5.94 (s, 0.2H), 6.14 (s, 0.8 H), 7.23−7.34 (br m, 2H), 7.43−7.66 (br m, 1.2H), 7.72 (s, 0.8H). The filtrate was concentrated, and the resulting waxy yellow solid was triturated with hexanes (50 mL) to give a white solid (1.4 g, 6%). ^{1}H NMR (300 MHz, DMSO-d_6/TFA-d) δ 2.13 (s, 2.4H), 2.49 (s, 0.6), 5.94 (s, 0.8H), 6.14 (s, 0.2H), 7.23−7.34 (br m, 2H), 7.43−7.66 (br m, 1.8H), 7.72 (s, 0.2H).

To a suspension of 3-(3-bromophenyl)but-2-enoic acid (mixed isomers) (16.2 g, 67.3 mmol) in 250 mL of methylene chloride was added oxalyl chloride (7.10 mL, 80.8 mmol) followed by DMF (260 μL, 3.37 mmol), and the reaction was stirred at room temperature. After 2 h the solvent was removed under reduced pressure to give the title compound as a light pink solid (17.0 g, 97%). ^{1}H NMR (300 MHz, $CDCl_3$) δ 2.22 (s, 2.4H); 2.51 (s, 0.6H); 6.25 (s, 0.2H); 6.44 (s, 0.8H); 7.32 (m, 1H); 7.42 (d, J = 6.9 Hz, 1H); 7.56 (d, J = 6.9 Hz, 1H); 7.58 (s, 1H).

5-(3-Bromophenyl)-3-methylpent-2-enoyl Chloride (19b). To **18b** was added a solution of trifluroracetic acid:dichloromethane

(1:1, 100 mL), and the reaction was stirred at room temperature for 15 min. The solvents were removed under reduced pressure, and the resulting solid was triturated with hexanes (100 mL). The mixture was filtered and the solid dried under reduced pressure to give 5-(3-bromophenyl)-3-methylpent-2-enoic acid as a white solid (18.48 g, 84%) yield over two steps. ^{1}H NMR (300 MHz, DMSO-d_6) δ 1.88 (d, J = 1.3 Hz, 1H), 2.14 (d, J = 1.1 Hz, 2H), 2.43 (t, J = 8.1 Hz, 2H), 2.71−2.80 (m, 2H), 5.62 (d, J = 1.1 Hz, .5H), 5.66 (s, 5H), 7.25 (d, J = 4.5 Hz, 2H), 7.35−7.42 (m, 1H), 7.47 (s, 1H).

To a 0 °C stirred solution of 5-(3-bromophenyl)-3-methylpent-2-enoic acid (18.5 g, 68.7 mmol) in dichloromethane (100 mL) was added oxalyl chloride (7.2 mL, 82.10 mmol) followed by *N*,*N*-dimethylformamide (0.266 mL, 3.43 mmol), and the reaction was stirred at 0 °C for 1 h and allowed to warm to room temperature. After 1 h the solvent was removed under reduced pressure to give the title compound as a cloudy oil, which was immediately carried forward into the next reaction (21.78 g, 110%).

3-(3-bromophenyl)-*N*-cyano-*N*-methylbut-2-enamide (20a). To a solution of cyanogen bromide (4.24 g, 40.0 mmol) (TOXIC!) in 100 mL of THF at −60 °C was added sodium carbonate (6.36 g, 60.0 mmol) followed by dropwise addition of a solution of 2.0 M methylamine solution in THF (20 mL 40 mmol). The bath temperature was kept below −20 °C for 2 h. The reaction was filtered cold through a pad of Celite under nitrogen. A solution of **19a** (single isomer) (5.19 g, 20.0 mmol) in 100 mL of THF was added to the filtrate. To this mixture was added *N*,*N*-diisopropylethylamine (4.2 mL, 24 mmol), the reaction was stirred at room temperature for 2 h, and the solvents were removed under reduced pressure. The crude compound was purified using flash chromatography on silica gel eluting with DCM to give the title compound as an off-white solid (4.29 g, 75%). ^{1}H NMR (300 MHz, DMSO-d_6) δ 2.44 (s, 3H); 3.22 (s, 3H); 6.65 (s, 1H); 7.42 (t, J = 7.8 Hz, 1H); 7.58 (d, J = 8.4 Hz, 1H); 7.65 (d, J = 7.8 Hz, 1H); 7.76 (t, J = 1.8 Hz, 1H).

5-(3-Bromophenyl)-*N*-cyano-*N*,3-dimethylpent-2-enamide (20b). To a −78 °C stirred solution of cyanogen bromide (14.6 g, 0.137 mmol) (TOXIC!) in tetrahydrofuran (100 mL) was added sodium carbonate (21.8 g, 0.206 mmol) followed by dropwise addition of a solution of methylamine in THF (2.00 M, 68.7 mL, 0.137 mol). The mixture was stirred at −78 °C for 1.5 h. The reaction was filtered cold through Celite under a blanket of nitrogen and a solution of **19b** (19.75 g (theoretical), 0.0686 mmol theoretical) in THF (100 mL) was added to the filtrate. To this mixture was added *N*,*N*-diisopropylethylamine (14.4 mL, 82.0 mol), reaction stirred at room temperature for 2 h, and the solvents were removed under reduced pressure. The crude compound was purified on silica gel (0.5 kg) in a large filter funnel eluting with dichloromethane to give the title compound as a tan solid (16.6 g, 79%). ^{1}H NMR (300 MHz, DMSO-d_6) δ 1.99 (d, J = 1.3 Hz, 1H), 2.14 (d, J = 1.1 Hz, 2H), 2.52 (dd, J = 3.8, 2.0 Hz, 2H), 2.79 (t, J = 7.7 Hz, 2H), 3.13 (s, 3H), 6.22 (d, J = 6.6 Hz, 1H), 7.24−7.27 (m, 2H), 7.37−7.41 (m, 1H), 7.49 (s, 1H); MS (APCI+) m/z 307 $[M + 1]^+$.

6-(3-Bromophenyl)-1-(4-methoxybenzylamino)-3,6-dimethyl-5,6-dihydro-3*H*-pyrimidin-4-one (21a) To a solution of **20a** prepared from multiple batches with both isomers (12.8 g, 45.7 mmol) in 50 mL of DMF was added 4-methoxybenzylamine (14.9 mL, 114 mmol). After 4 h the solvent was removed under reduced pressure. The crude compound was purified by flash chromatography on silica gel eluting with DCM, 2.5% MeOH/DCM, 5% MeOH/DCM followed by a second flash chromatography on silica gel eluting with Et_2O, EtOAc, 5% MeOH/EtOAc, 10% MeOH/EtOAc to afford the title compound as an off white-solid (15.4 g, 81%). ^{1}H NMR (300 MHz, DMSO-d_6/TFA-d) δ 1.65 (s, 3H), 3.20 (s, 3H), 3.30 (d, J = 16.5 Hz, 1H), 3.58 (d, J = 16.8 Hz, 1H), 3.78 (s, 3H), 4.97 (dd, J = 4.8 Hz, 2H), 6.96 (d, J = 8.7 Hz, 2H), 7.34 (m, 4H), 7.57 (m, 2H); MS (APCI+) m/z 416 $[M + H]^+$; LC Method A: t_R = 1.80 min.

6-(3-Bromophenethyl)-1-(4-methoxybenzyl)-tetrahydro-2-imino-3,6-dimethylpyrimidin-4(1*H*)-one (21b). To a stirred solution of **20b** (15.0 g, 48.8 mmol) in *N*,*N*-dimethylformamide (50 mL) was added 4-methoxybenzylamine (12.8 mL, 97.7 mmol). After 4 h, the solvent was removed under reduced pressure, and the crude compound was purified by flash chromatography on a 6″ × 8″ silica gel column eluting with 5% MeOH/DCM to give the title compound as an amber gum (20.4 g, 94%). ^{1}H NMR (300 MHz, DMSO-d_6/TFA-d) δ 1.34 (s, 3H), 1.93 (m, 2H), 2.55−2.64 (m, 2H), 3.05 (dd, J = 24.0, 16.8 Hz, 2H), 3.27 (s, 3H), 3.80 (s, 3H), 4.87 (dd, J = 36.4, 18.5 Hz, 2H), 6.97 (d, J = 8.6 Hz, 1H), 7.14−7.34 (m, 6H), 7.38 (d, J = 1.6 Hz, 1H); MS (APCI+) m/z 444 $[M + 1]^+$.

2-Amino-6-(3-bromophenyl)-3,6-dimethyl-5,6-dihydro-3*H*-pyrimidin-4-one (22a). To a solution of **21a** (15.5 g, 37.1 mmol) in 150 mL of acetonitrile was added 50 mL of water followed by ceric ammonium nitrate (61.1 g, 111 mmol), and the reaction stirred for 18 h. Celite (32 g) was added followed by sodium bicarbonate (31.2 g, 371 mmol), and reaction was stirred for 1 h. Additional Celite (15 g) was added and the mixture stirred for an additional 1 h. The reaction was filtered through Celite and the filtrate concentrated under reduced pressure. A crude purification was performed using silica gel eluting with 15:85:0.1 MeOH:DCM:acetic acid. The resulting orange solid was triturated with methanol to give the first batch of the title compound. The solvents were removed from the filtrate under reduced pressure, and the resulting orange solid was triturated with ethanol to give a second batch of the title compound. The batches were combined to give the title compound as an off-white solid (8.75 g, 79%). ^{1}H NMR (300 MHz, DMSO-d_6/TFA-d) δ 1.64 (s, 3H), 3.14 (s, 3H), 3.19 (d, J = 16.5 Hz, 1H), 3.49 (d, J = 16.2 Hz, 1H), 7.39 (m, 2H), 7.55 (m, 1H), 7.67 (s, 1H): MS (APCI+) m/z 296 $[M + H]^+$;

6-(3-Bromophenethyl)-2-amino-5,6-dihydro-3,6-dimethylpyrimidin-4(3*H*)-one (22b). To a solution of **21b** (20.3 g, 45.6 mmol) in acetonitrile (132 mL) was added water (33 mL) followed by ceric ammonium nitrate (75.0 g, 137 mmol), and the reaction was stirred for 18 h. Celite (40 g) was added followed by sodium bicarbonate (38.0 g, 452 mmol), and the reaction was stirred for 1 h. Additional Celite (20 g) was added, the reaction filtered through Celite washing with acetonitrile, and the filtrate concentrated under reduced pressure. Ethanol was added to the residue, the solids were removed by filtration, and solvent was removed under reduced pressure. The resulting solids were triturated with diethyl ether, and the solid material was dried under reduced pressure. This material was partitioned between ethyl acetate (500 mL) and a saturated sodium chloride/water solution (1:1, 500 mL). The organic layer was washed with saturated sodium chloride and dried over sodium sulfate, and the solvents were removed under reduced pressure. The crude material was purified by flash chromatography on a 6 in. × 8 in. silica gel column eluting with dichloromethane:methanol:acetic acid (90:10:0.1 to afford the title compound as a tan solid (13.3 g, 90%). ^{1}H NMR (300 MHz, DMSO-d_6/TFA-d) δ 1.33 (s, 3H), 1.86 (m, 2H), 2.64 (t, J = 8.5 Hz, 2H), 2.79 (d, J = 16.4 Hz, 1H), 2.94 (d, J = 16.4 Hz, 1H), 3.20 (s, 3H), 7.26 (d, J = 5.0 Hz, 2H), 7.40 (td, J = 4.5, 1.9 Hz, 1H), 7.49 (s, 1H); MS (APCI+) m/z 324 $[M + 1]^+$.

2-Amino-3,6-dimethyl-6-phenyl-5,6-dihydro-3*H*-pyrimidin-4-one (23). To a solution of **22a** (100 mg, 0.338 mmol) and triethylamine (103 mg, 1.01 mmol) in MeOH (34 mL) was added palladium hydroxide (40 mg). The mixture was charged with hydrogen (50 psi) and shaken on a Parr shaker for 2 h. The reaction was filtered through Celite and the filtrate concentrated under reduced pressure. The crude compound was purified using Method C to afford the title compound as a white TFA salt (8 mg, 10%). ^{1}H NMR (300 MHz, DMSO-d_6/TFA-d) δ 1.63 (s, 3H), 3.08 (s, 3H), 3.18 (d, J = 16.5 Hz, 1H), 3.42 (d, J = 16.5 Hz, 1H), 7.42 (m, 5H); MS (APCI+) m/z 218 $[M + H]^+$; HRMS (TOF) m/z calcd for $C_{12}H_{15}N_3O$ $[M + H]^+$, 218.1288; found, 218.1293.

2-Amino-6-(3′-methoxybiphenyl-3-yl)-3,6-dimethyl-5,6-dihydro-3*H*-pyrimidin-4-one (24). To a solution of **22a** (47.0 mg, 0.132 mmol) in 1.5 mL of 7:3:2 1,2-dimethoxyethane:water:ethanol were added cesium carbonate (129 mg, 0.396 mmol), 3-methoxyphenylboronic acid (26.0 mg, 0.172 mmol), and dichlorobis(triphenylphosphine)palladium(II) (4.6 mg, 0.0065 mmol). The reaction

was heated by microwave for 15 min at 150 °C after which the solvents were removed under a stream of nitrogen. To the resulting brown gum was added ACN:water:TFA (75:25:0.1, 2.0 mL), and the precipitate was removed. The filtrate was purified using Method C to afford the title compound as a white TFA salt (25 mg, 43%). ^{1}H NMR (300 MHz, DMSO-d_6/TFA-d) δ 1.71 (s, 3H), 3.13 (s, 3H), 3.21 (d, J = 16.5 Hz, 1H), 3.59 (d, J = 16.2 Hz, 1H), 3.85 (s, 3H), 6.98 (d, J = 3.9 Hz, 1H), 7.23 (m, 2H), 7.41 (m, 2H), 7.51 (t, J = 7.8 Hz, 1H), 7.64 (d, J = 7.5 Hz, 1H), 7.71 (s, 1H); MS (APCI+) m/z 324 $[M + H]^+$; HRMS (TOF) m/z calcd for $C_{19}H_{21}N_3O_2$ $[M + H]^+$, 324.1707; found, 324.1718.

2-Amino-6-[2-(3′-methoxybiphenyl-3-yl)ethyl]-3,6-dimethyl-5,6-dihydro-3*H*-pyrimidin-4-one (27). This material was prepared according to the method described for **24** using **22b** and 3-methoxyphenylboronic acid to afford the title compound as a white TFA salt (65 mg, 45%). ^{1}H NMR (300 MHz, DMSO-d_6/TFA-d) δ 1.37 (s, 3H), 1.94 (m, 2H), 2.71 (m, 2H), 2.82 (d, J = 16.4 Hz, 1H), 2.98 (d, J = 16.4 Hz, 1H), 3.21 (s, 3H), 3.84 (s, 3H), 6.95 (dd, J = 8.0, 2.2 Hz, 1H), 7.19 (d, J = 2.2 Hz, 1H), 7.23 (t, J = 6.9 Hz, 2H), 7.38 (t, J = 7.9 Hz, 2H), 7.51 (m, 2H); MS (ES+) m/z 352 $[M + H]^+$; HRMS (TOF) m/z calcd for $C_{21}H_{25}N_3O$-$_2$ $[M + H]^+$, 352.2020; found, 352.2019.

(*S*)-2-Amino-6-[2-(3′-methoxybiphenyl-3-yl)ethyl]-3,6-dimethyl-5,6-dihydro-3*H*-pyrimidin-4-one (28). To **27**, 165 mg, was added methanol, and the enantiomers were separated on a preparative supercritical fluid chromatography system using Method F. The solvent was removed from the product fractions using a Genevac evaporator to give a waxy solid. This solid was then purified using Method C. The combined purified fractions were lyophilized to give the title compound as a white TFA salt (28.9 mg, 18%). ^{1}H NMR (300 MHz, DMSO-d_6/TFA-d) δ 1.36 (s, 3H), 1.93 (t, J = 8.5 Hz, 2H), 2.70 (t, J = 8.9 Hz, 2H), 2.82 (d, J = 16.4 Hz, 1H), 2.97 (d, J = 16.4 Hz, 1H), 3.20 (s, 3H), 3.84 (s, 3H), 6.95 (dd, J = 8.1, 2.0 Hz, 1H), 7.18 (d, J = 2.2 Hz, 2H), 7.23 (t, J = 6.9 Hz, 3H), 7.38 (t, J = 7.9 Hz, 2H), 7.51 (t, J = 7.7 Hz, 2H); MS (APCI+) m/z 352 $[M + H]^+$; SFC Method G, t_R = 5.18 min, >99% pure, >99% ee; HRMS (TOF) m/z calcd for $C_{21}H_{25}N_3O_2$ $[M + H]^+$, 352.2020; found, 352.2023.

(*R*)-2-Amino-6-[2-(3′-methoxybiphenyl-3-yl)ethyl]-3,6-dimethyl-5,6-dihydro-3*H*-pyrimidin-4-one (29). This enantiomer was isolated from the chiral purification of **28** and afforded the title compound as a white TFA salt (36.2 mg, 22%). ^{1}H NMR (300 MHz, DMSO-d_6/TFA-d) δ 1.36 (s, 3H), 1.93 (t, J = 8.5 Hz, 2H), 2.71 (t, J = 14.7 Hz, 2H), 2.82 (d, J = 16.4 Hz, 1H), 2.97 (d, J = 16.4 Hz, 1H), 3.20 (s, 3H), 3.84 (s, 3H), 6.95 (dd, J = 8.1, 2.0 Hz, 1H), 7.18 (d, J = 2.2 Hz, 1H), 7.23 (t, J = 6.9 Hz, 2H), 7.38 (t, J = 7.9 Hz, 2H), 7.51 (t, J = 7.7 Hz, 2H); MS (APCI+) m/z 352 $[M + H]^+$; SFC Method G, t_R = 4.36 min, >99% pure, >99% ee; HRMS (TOF) m/z calcd for $C_{21}H_{25}N_3O$-$_2$ $[M + H]^+$, 352.2020; found, 352.2025.

Crystallography. Recombinant human BACE-1 residues 14−453 was produced in bacteria as inclusion bodies and refolded using a method described previously.[47] Crystals of apo-BACE-1 suitable for ligand soaking were obtained by a procedure described by Patel et al.[47] In brief, BACE-1 was buffer exchanged into 20 mM Tris (pH 8.2), 150 mM NaCl, 1 mM DTT and concentrated to 8 mg/mL. DMSO (3% v/v) was added to the protein prior to crystallization. Apo-BACE-1 crystals were grown using the hanging drop vapor diffusion method at 20 °C. Protein was mixed with an equal volume of mother liquor containing 20−22.5% (w/v) PEG 5000 monomethylethyl (MME), 200 mM sodium citrate (pH 6.6), and 200 mM ammonium iodide. Crystals were cryoprotected for data collection by brief immersion in 30% PEG 5000 MME, 100 mM sodium citrate (pH 6.6), 200 mM ammonium iodide, and 20% (v/v) glycerol. For inhibitor soaking, 0.5−0.1 M DMSO stock solutions were made. A 10-fold dilution of the compound stock solution in a stabilization solution (33% (w/v) PEG 5000 monomethylethyl (MME), 110 mM sodium citrate (pH 6.6), and 220 mM ammonium iodide was made. Crystals were added to the soaking solution for up to 6 h prior to flash freezing and data collection. Data were collected at a number of synchrotron beam lines at the European Synchrotron Radiation Facility, Grenoble, France and Synchrotron Radiation Source, Daresbury, U.K. All data sets were processed with MOSFLM[50] and scaled using SCALA.[51] Structure solution and initial refinement of the protein−ligand complexes were carried out on our automated scripts using a modified apo-BACE-1 structure (PDB id code 1w50) as a starting model. Bound ligands were automatically identified and fitted into $F_o - F_c$ electron density using AutoSolve52 and further refined using automated scripts followed by rounds of rebuilding in AstexViewer2[53] and refinement using Refmac.[54] Data collection and refinement statistics for selected crystal structures are presented in Table 2.

Biology. This section describes the various assays used to assess the inhibition of BACE-1 by the compound reported in this paper. In several of the assays up to 5% DMSO was used to ensure complete solubility of the test compound. Appropriate control experiments demonstrated that the levels of DMSO used had no detrimental effects on the inhibition values generated.

Preparation of BACE-1. The BACE-1 used in most assays was expressed in *Escherichia coli* and purified as previously described.[40] The stock solution of BACE-1 was 1 mg/mL in 20 mM Tris, 150 mM NaCl, and 1 mM DTT at pH 8.2. The BACE-1 used for the SPR assay of compounds **5**−**7** was prepared according to the procedure of Lullau et al.[55]

BACE-1 SPR Assay. Sensor Chip Preparation: BACE-1 was assayed on a Biacore3000 instrument by attaching either a peptidic transition state isostere (TSI) or a scrambled version of the peptidic TSI to the surface of a BIAcore CM5 sensor chip. The peptides, KFES-statine-ETIAEVENV and KTEEISEVN-statine-VAEF, were purchased from the Synpep Corporation and BioSource, respectively. The scrambled peptide KFES-statine-ETIAEVENV was coupled to channel 1, and the TSI inhibitor KTEEISEVN-statine-VAEF was coupled to channel 2 of the same chip using the following protocol. The two peptides were dissolved at 0.2 mg/mL in 20 mM sodium acetate pH 4.5, and then the solutions were centrifuged at 14K rpm to remove any particulates. Carboxyl groups on the dextran layer of the chip were activated by injecting a 1:1 mixture of 0.5 M *N*-ethyl-*N*′-(3-dimethylaminopropyl)carbodiimide (EDC) and 0.5 M *N*-hydroxysuccinimide (NHS) at 5 μL/min for 7 min. The stock solution of the control peptide was injected in channel 1 for 7 min at 5 μL/min, and the remaining carboxyl groups were blocked by injecting 1 M ethanolamine for 7 min at 5 μL/min. The TSI peptide was coupled to channel 2 in the same manner. Assay Protocol: The running buffer for the BACE-1 SPR assay consisted of 25 mM sodium acetate, 200 mM NaCl, 0.005% SP20, and 5% DMSO at pH 4.5. The stock solution of BACE-1 was diluted to 0.5 μM in running buffer minus DMSO. The diluted BACE-1 was mixed with DMSO or compound dissolved in DMSO to achieve a final DMSO concentration of 5%. The mixing was done in a 96-well plate that was then sealed and maintained at 4 °C for 1 h. The mixture was then injected over channels 1 and 2 of the CM5 BIAcore chip at a rate of 20 μL/min, and the signal was recorded in response units (RU). Specific binding of BACE-1 to the TSI inhibitor was monitored on channel 2, while any binding to channel 1 was nonspecific and was subtracted from the channel 2 response. BACE-1 binding to the chip was quantified by measuring the rate of the increase in response 20 s after injection. The DMSO control was defined as 100% binding, and the effect of the inhibitor was reported as percent inhibition of the DMSO control.

FRET Assay Protocol. The enzymatic activity of BACE-1 was measured with an internally quenched fluorescent substrate, E(edans)ISEVNLDAEFK(dabcyl) purchased from BioSource. Cleavage of the substrate resulted in a fluorescent product that was measured on a Wallac Victor II plate reader with an excitation wavelength of 360 nm and an emission wavelength of 485 nm. A 4 mM stock solution of substrate was prepared in 45 mM Tris, 45 mM borate, and 1 mM EDTA at pH 8.2. BACE-1 was diluted 1:70 in 40 mM MES pH 5.0, and substrate was diluted to 30 μM in the same buffer. Enzyme and substrate stock solutions were kept on ice until the assay was initiated. The assay was done in a 384-well plate with a final reaction volume of 20 μL. Enzyme (9 μL) was added to the plate, and then 1 μL of compound in DMSO was added and

preincubated for 5 min. Substrate (10 μL) was added, and the reaction proceeded in the dark for 1 h at room temperature. The final dilution of enzyme was 1:140; the final concentration of substrate was 15 μM (K_m of 25 μM). BACE-1 activity in the presence of DMSO alone defined the 100% activity level, and 0% activity was defined by completely inhibiting BACE-1 with 1 μM of a TSI inhibitor (KTEEISEVN-sta-VAEF).

IGEN Assay. Assay Protocol: BACE-1 activity was also quantified with a nonfluorescent substrate, and the product of the reaction was measured with a technology developed by Bioveris. The nonfluorescent assay was run as follows. BACE-1 was diluted 1:100 in 40 mM MES pH 5.0, and a 2 mM stock solution of Biotin-TEEISEVNLDAEFRHDS (purchased from Synpep Corporation) was diluted to 12 μM in the same buffer. DMSO stock solutions of compounds or DMSO alone were diluted to the desired concentration in 40 mM MES pH 5.0. Compound in DMSO (3 μL) was added to the plate followed by 27 μL of BACE-1, and then the mixture preincubated for 5 min. The reaction was started by adding 30 μL of substrate. The final dilution of enzyme was 1:200; the final concentration of substrate was 6 μM (K_m is 150 μM). After a 20 min reaction at room temperature, the reaction was stopped by removing 10 μL of the reaction mix and diluting it 1:25 in 0.20 M Tris pH 8.0. Addition of DMSO alone defined 100% BACE-1 activity while 1 μM KTEEISEVN-sta-VAEF was used to define 0% activity. Product Measurement with Bioveris Technology: The biotin-labeled product was captured with streptavidin-coated Dynabeads and then quantified with a custom-made rabbit polyclonal antibody (Zymed) made to recognize the Swedish mutant neoepitope formed after BACE-1 cleavage. The Bioveris technology is based on the electrochemiluminescence of ruthenium-based proprietary labels, which in this case was covalently attached to a goat anti-rabbit antibody (Ru-GAR) purchased from Jackson ImmunoResearch Labs. The Ru-GAR was made according to the protocol suggest by the manufacturer. Briefly, the Ru label and antibody were mixed at a 10:1 challenge ratio and then incubated for 1 h. The reaction was quenched with 2 M glycine and the excess label removed by gel filtration over a NAP 5 column from Amersham Biosciences. Quantification was done as described below. All antibodies and the streptavidin-coated Dynabeads were diluted into Dulbecco-PBS containing 0.5% bovine serum albumin and 0.5% Tween-20. The product was quantified by adding 50 μL of a 1:5000 dilution of the neoepitope antibody to 50 μL of the 1:25 dilution of the BACE-1 reaction mixture. Then, 100 μL of Dulbecco-PBS (0.5% BSA, 0.5% Tween-20) containing 0.2 mg/mL IGEN beads and a 1:5000 dilution of the Ru-GAR antibody were added. The final dilution of neoepitope antibody was 1:20 000, the final dilution of Ru-GAR was 1:10 000, and the final concentration of beads was 0.1 mg/mL. The mixture is read on a Bioveris M8 Analyzer after a 2 h incubation at room temperature.

BACE-1 Cellular Assay. Generation of HEK-Fc33-1 Cell Line: The cDNA encoding full length BACE-1 was fused in frame with a three amino acid linker (Ala-Val-Thr) as described by Vassar et al.[9] to the Fc portion of the human IgG1 starting at amino acid 104. The BACE-1-Fc construct was then cloned into a GFP/pGEN-IRES-neoK vector (a proprietary vector of AstraZeneca) for protein expression in mammalian cells. The expression vector was stably transfected into HEK-293 cells using the calcium phosphate method. Colonies were selected with 250 μg/mL of geneticin sulfate (G-418). Limited dilution cloning was performed to generate homogeneous cell lines. Clones were characterized by levels of APP expression and Aβ1−40 secreted in the conditioned media using an ELISA assay. Aβ1−40 secretion of BACE-1/Fc clone Fc33−1 was moderate. Cell Culture: HEK293 cells stably expressing human BACE-1 (HEK-Fc33−1) were grown at 37 °C in Dulbecco's modified Eagle's medium (DMEM) containing 10% heat-inhibited FBS, 0.5 mg/mL antibiotic-antimycotic solution, and 0.05 mg/mL G-418. Aβ1−40 Release Assay: Cells were harvested when between 80 and 90% confluent. An amount of 100 μL of cells at a cell density of 1.5×10^6/mL were added to a white 96-well cell culture plate with clear flat bottom, or a clear, flat-bottom 96-well cell culture plate, containing 100 μL of inhibitor in cell culture medium with DMSO at a final concentration of 1%. After the plate was incubated at 37 °C for 24 h, 100 μL of cell medium was transferred to a round-bottom 96-well plate to quantify Aβ1−40 levels. The cell culture plates were saved for ATP assay as described below. To each well of the round-bottom plate, 50 μL of detection solution containing 0.2 mg/mL RaAb40 (BioSource) and 0.25 μg/mL biotin-4G8 (Signet) (prepared in Dulbecco's phosphate-buffered saline (DPBS) with 0.5%BSA and 0.5% Tween-20) was added and incubated at 4 °C for >7 h. Then a 50 μL solution (prepared in the same buffer as above) containing 0.062 mg/mL Ru-GAR and 0.125 mg/mL Dynabeads were added per well. The solutions in the round-bottom plate were shaken at room temperature on a plate shaker for 1 h, and the plates were then measured for electrochemiluminescence counts in a Bioveris M8 Analyzer. Aβ1−40 standard curves were obtained with two-fold serial dilution of an Aβ1−40 stock solution of known concentration in the same cell culture medium used in cell-based assays. ATP Assay: As indicated above, after transferring 100 μL of medium from cell culture plates for Aβ1−40 detection, the plates, which still contained cells, were saved for cytotoxicity assays by using the assay kit (ViaLight Plus) from Cambrex BioScience that measures total cellular ATP. Briefly, to each well of the plates, 50 μL of cell lysis reagent was added. The plates were incubated at room temperature for 10 min. Two minutes following addition of 100 μL reconstituted ViaLight Plus reagent for ATP measurement, the luminescence of each well was measured in an LJL Analyst or Wallac Victor II plate reader.

Acknowledgment. We wish to thank Dr. Christof Angst for his support and encouragement during the course of this work, and Dr. Todd Brugel for helpful suggestions in the preparation of this manuscript.

Supporting Information Available: Detailed description of HPLC methods, HPLC purity analysis of final compounds, and experimental procedures for compounds **8b**, **8d**, **8f**, **9a**, **9d**−**f**, **10b**−**d**, **11b**,**c**, **12c**, **13a**−**c**, **25**, and **26**. This material is available free of charge via the Internet at http://pubs.acs.org.

References

(1) Herbert, L. E.; Scherr, P. A.; Bienias, J. L.; Bennett, D. A.; Evans, D. A. Alzheimer Disease in the U.S. population: prevalence estimates using the 2000 census. *Arch. Neurol.* **2003**, *60*, 1119−1122.

(2) Losing a million minds: confronting the tragedy of Alzheimer's Disease and other dementias. U.S. Congress Office of Technology Assessment; U.S. Goverment Printing Office: Washington, DC, 1987; p 14.

(3) *Alzheimer's Disease medications fact sheet*, NIH Publication No.03−3431; Alzheimer's Disease Education and Referral Center: Silver Spring, MD, 2006; pp 1−6.

(4) Hardy, J.; Selkoe, D. J. The amyloid hypothesis of Alzheimer's disease: progress and problems on the road to therapeutics. *Science* **2002**, *297*, 353−356.

(5) Sinha, S.; Lieberburg, I. Cellular mechanisms of β-amyloid production and secretion. *Proc. Natl. Acad. Sci. U.S.A.* **1999**, *96*, 11049−11053.

(6) Hussain, I.; Powell, D.; Howlett, D. R.; Tew, D. G.; Meek, T. D.; Chapman, C.; Gloger, I. S.; Murphy, K. E.; Southan, C. D.; Ryan, D. M.; Smith, T. S.; Simmons, D. L.; Walsh, F. S.; Dingwall, C.; Christie, G. Identification of a Novel Aspartic Protease (Asp 2) as β-Secretase. *Mol. Cell Neurosci.* **1999**, *14*, 419−427.

(7) Lin, X.; Koelsch, G.; Wu, S.; Downs, D.; Dashti, A.; Tang, J. Human aspartic protease memapsin 2 cleaves the β-secretase site of β-amyloid precursor protein. *Proc. Natl. Acad. Sci. U.S.A.* **2000**, *97*, 1456−1460.

(8) Sinha, S.; Anderson, J. P.; Barbour, R.; Basi, G. S.; Caccavello, R.; Davis, D.; Doan, M.; Dovey, H. F.; Frigon, N.; Hong, J.; Jacobson-Croak, K.; Jewett, N.; Keim, P.; Knops, J.; Lieberburg, I.; Power, M.; Tan, H.; Tatsuno, G.; Tung, J.; Schenk, D.; Seubert, P.; Suomensaari, S. M.; Wang, S.; Walker, D.; Zhao, J.; McConlogue, L.; John, V. Purification and cloning of amyloid precursor protein β-secretase from human brain. *Nature* **1999**, *402*, 537−540.

(9) Vassar, R.; Bennett, B. D.; Babu-Khan, S.; Kahn, S.; Mendiaz, E. A.; Denis, P.; Teplow, D. B.; Ross, S.; Amarante, P.; Loeloff, R.; Luo, Y.; Fisher, S.; Fuller, J.; Edenson, S.; Lile, J.; Jarosinski, M. A.; Biere, A. L.; Curran, E.; Burgess, T.; Louis, J.-C.; Collins, F.; Treanor, J.; Rogers, G.; Citron, M. β-Secretase cleavage of Alzheimer's amyloid precursor protein by the transmembrane aspartic protease BACE. *Science* **1999**, *286*, 735−741.

(10) Cumming, J. N.; Iserloh, U.; Kennedy, M. E. Design and development of BACE-1 inhibitors. *Curr. Opin. Drug Discovery Dev.* **2004**, *7*, 536−556.
(11) John, V.; Beck, J. P.; Bienkowski, M. J.; Sinha, S.; Heinrikson, R. L. Human β-Secretase (BACE) and BACE Inhibitors. *J. Med. Chem.* **2003**, *46*, 4625−4630.
(12) Durham, T. B.; Shepherd, T. A. Progress toward the discovery and development of efficacious BACE inhibitors. *Curr. Opin. Drug Discovery Dev.* **2006**, *9*, 776−791.
(13) Baxter, E. W.; Reitz, A. B. BACE inhibitors for the treatment of Alzheimer's disease. *Annu. Rep. Med. Chem.* **2005**, *40*, 35−48.
(14) Schmidt, B.; Baumann, S.; Braun, H. A.; Larbig, G. Inhibitors and modulators of β- and γ-secretase. *Curr. Top. Med. Chem.* **2006**, *6*, 377−392.
(15) Guo, T.; Hobbs, D. W. Development of BACE-1 inhibitors for Alzheimer's disease. *Curr. Med. Chem.* **2006**, *13*, 1811−1829.
(16) Chen, S.-H.; Lamar, J.; Guo, D.; Kohn, T.; Yang, H.-C.; McGee, J.; Timm, D.; Erickson, J.; Yip, Y.; May, P.; McCarthy, J. P3 cap modified Phe*-Ala series BACE inhibitors. *Bioorg. Med. Chem. Lett.* **2004**, *14*, 245−250.
(17) Lamar, J.; Hu, J.; Bueno, A. B.; Yang, H.-C.; Guo, D.; Copp, J. D.; McGee, J.; Gitter, B.; Timm, D.; May, P.; McCarthy, J.; Chen, S.-H. Phe*-Ala-based pentapeptide mimetics are BACE inhibitors: P2 and P3 SAR. *Bioorg. Med. Chem. Lett.* **2004**, *14*, 239−243.
(18) Hu, B.; Fan, K. Y.; Bridges, K.; Chopra, R.; Lovering, F.; Cole, D.; Zhou, P.; Ellingboe, J.; Jin, G.; Cowling, R.; Bard, J. Synthesis and SAR of bis-statine based peptides as BACE 1 inhibitors. *Bioorg. Med. Chem. Lett.* **2004**, *14*, 3457−3460.
(19) Ghosh, A. K.; Devasamudram, T.; Hong, L.; DeZutter, C.; Xu, X.; Weerasena, V.; Koelsch, G.; Bilcer, G.; Tang, J. Structure-based design of cycloamide-urethane-derived novel inhibitors of human brain memapsin 2 (β-secretase). *Bioorg. Med. Chem. Lett.* **2005**, *15*, 15−20.
(20) Ghosh, A. K.; Bilcer, G.; Harwood, C.; Kawahama, R.; Shin, D.; Hussain, K. A.; Hong, L.; Loy, J. A.; Nguyen, C.; Koelsch, G.; Ermolieff, J.; Tang, J. Structure-based design: potent inhibitors of human brain memapsin 2 (β-secretase). *J. Med. Chem.* **2001**, *44*, 2865−2868.
(21) Hom, R. K.; Fang, L. Y.; Mamo, S.; Tung, J. S.; Guinn, A. C.; Walker, D. E.; Davis, D. L.; Gailunas, A. F.; Thorsett, E. D.; Sinha, S.; Knops, J. E.; Jewett, N. E.; Anderson, J. P.; John, V. Design and synthesis of statine-based cell-permeable peptidomimetic inhibitors of human β-secretase. *J. Med. Chem.* **2003**, *46*, 1799−1802.
(22) Hom, R. K.; Gailunas, A. F.; Mamo, S.; Fang, L. Y.; Tung, J. S.; Walker, D. E.; Davis, D.; Thorsett, E. D.; Jewett, N. E.; Moon, J. B.; John, V. Design and synthesis of hydroxyethylene-based peptidomimetic inhibitors of human β-secretase. *J. Med. Chem.* **2004**, *47*, 158−164.
(23) Yang, W.; Lu, W.; Lu, Y.; Zhong, M.; Sun, J.; Thomas, A. E.; Wilkinson, J. M.; Fucini, R. V.; Lam, M.; Randal, M.; Shi, X.-P.; Jacobs, J. W.; McDowell, R. S.; Gordon, E. M.; Ballinger, M. D. Aminoethylenes: a tetrahedral intermediate isostere yielding potent inhibitors of the aspartyl protease BACE-1. *J. Med. Chem.* **2006**, *49*, 839−842.
(24) Brady, S. F.; Singh, S.; Crouthamel, M.-C.; Holloway, M. K.; Coburn, C. A.; Garsky, V. M.; Bogusky, M.; Pennington, M. W.; Vacca, J. P.; Hazuda, D.; Lai, M.-T. Rational design and synthesis of selective BACE-1 inhibitors. *Bioorg. Med. Chem. Lett.* **2004**, *14*, 601−604.
(25) Hanessian, S.; Yun, H.; Hou, Y.; Yang, G.; Bayrakdarian, M.; Therrien, E.; Moitessier, N.; Roggo, S.; Veenstra, S.; Tintelnot-Blomley, M.; Rondeau, J.-M.; Ostermeier, C.; Strauss, A.; Ramage, P.; Paganetti, P.; Neumann, U.; Betschart, C. Structure-based design, synthesis, and memapsin 2 (BACE) inhibitory activity of carbocyclic and heterocyclic peptidomimetics. *J. Med. Chem.* **2005**, *48*, 5175−5190.
(26) Hong, L.; Koelsch, G.; Lin, X.; Wu, S.; Terzyan, S.; Ghosh, A. K.; Zhang, X. C.; Tang, J. Structure of the protease domain of memapsin 2 (β-secretase) complexed with inhibitor. *Science* **2000**, *290*, 150−153.
(27) Clark, D. E. Rapid calculation of polar molecular surface area and its application to the prediction of transport phenomena. 2. Prediction of blood-brain barrier penetration. *J. Pharm. Sci.* **1999**, *88*, 815−821.
(28) Lipinski, C. A.; Lombardo, F.; Dominy, B. W.; Feeney, P. J. Experimental and computational approaches to estimate solubility and permeability in drug discovery and development settings. *Adv. Drug Delivery Rev.* **2001**, *46*, 3−26.
(29) Hopkins, Andrew, L.; Groom, Colin, R.; Alex, A. Ligand efficiency: a useful metric for lead selection. *Drug. Discovery Today* **2004**, *9*, 430−431.
(30) Since IC_{50} values are dependent upon experimental conditions and are not a kinetic constant, the comparison of a LE value derived from an IC_{50} with a LE derived from a K_i is not strictly valid. However the differences are small. Since K_i values are generally lower than IC_{50} values, use of a K_i generally underestimates a LE relative to one derived from an IC_{50}.
(31) Stachel, S. J.; Coburn, C. A.; Steele, T. G.; Jones, K. G.; Loutzenhiser, E. F.; Gregro, A. R.; Rajapakse, H. A.; Lai, M.-T.; Crouthamel, M.-C.; Xu, M.; Tugusheva, K.; Lineberger, J. E.; Pietrak, B. L.; Espeseth, A. S.; Shi, X.-P.; Chen-Dodson, E.; Holloway, M. K.; Munshi, S.; Simon, A. J.; Kuo, L.; Vacca, J. P. Structure-based design of potent and selective cell-permeable inhibitors of human β-secretase (BACE-1). *J. Med. Chem.* **2004**, *47*, 6447−6450.
(32) Coburn, C. A.; Stachel, S. J.; Li, Y.-M.; Rush, D. M.; Steele, T. G.; Chen-Dodson, E.; Holloway, M. K.; Xu, M.; Huang, Q.; Lai, M.-T.; DiMuzio, J.; Crouthamel, M.-C.; Shi, X.-P.; Sardana, V.; Chen, Z.; Munshi, S.; Kuo, L.; Makara, G. M.; Annis, D. A.; Tadikonda, P. K.; Nash, H. M.; Vacca, J. P. Identification of a small molecule nonpeptide active site β-secretase inhibitor that displays a nontraditional binding mode for aspartyl proteases. *J. Med. Chem.* **2004**, *47*, 6117−6119.
(33) Garino, C.; Pietrancosta, N.; Laras, Y.; Moret, V.; Rolland, A.; Quelever, G.; Kraus, J.-L. BACE-1 inhibitory activities of new substituted phenyl-piperazine coupled to various heterocycles: Chromene, coumarin and quinoline. *Bioorg. Med. Chem. Lett.* **2006**, *16*, 1995−1999.
(34) Huang, D.; Luethi, U.; Kolb, P.; Cecchini, M.; Barberis, A.; Caflisch, A. In silico discovery of β-secretase inhibitors. *J. Am. Chem. Soc.* **2006**, *128*, 5436−5443.
(35) Huang, D.; Luethi, U.; Kolb, P.; Edler, K.; Cecchini, M.; Audetat, S.; Barberis, A.; Caflisch, A. Discovery of cell-permeable nonpeptide inhibitors of β-secretase by high-throughput docking and continuum electrostatics calculations. *J. Med. Chem.* **2005**, *48*, 5108−5111.
(36) Cole, D. C.; Manas, E. S.; Stock, J. R.; Condon, J. S.; Jennings, L. D.; Aulabaugh, A.; Chopra, R.; Cowling, R.; Ellingboe, J. W.; Fan, K. Y.; Harrison, B. L.; Hu, Y.; Jacobsen, S.; Jin, G.; Lin, L.; Lovering, F. E.; Malamas, M. S.; Stahl, M. L.; Strand, J.; Sukhdeo, M. N.; Svenson, K.; Turner, M. J.; Wagner, E.; Wu, J.; Zhou, P.; Bard, J. Acylguanidines as small-molecule β-secretase inhibitors. *J. Med. Chem.* **2006**, *49*, 6158−6161.
(37) Rajapakse, H. A.; Nantermet, P. G.; Selnick, H. G.; Munshi, S.; McGaughey, G. B.; Lindsley, S. R.; Young, M. B.; Lai, M.-T.; Espeseth, A. S.; Shi, X.-P.; Colussi, D.; Pietrak, B.; Crouthamel, M.-C.; Tugusheva, K.; Huang, Q.; Xu, M.; Simon, A. J.; Kuo, L.; Hazuda, D. J.; Graham, S.; Vacca, J. P. Discovery of oxadiazoyl tertiary carbinamine inhibitors of β-secretase (BACE-1). *J. Med. Chem.* **2006**, *49*, 7270−7273.
(38) Murray, C. W.; Callaghan, O.; Chessari, G.; Cleasby, A.; Congreve, M.; Frederickson, M.; Hartshorn, M. J.; McMenamin, R.; Patel, S.; Wallis, N. Application of fragment screening to β-secretase. *J. Med. Chem.* **2007**, *50*, 1116−1123.
(39) Congreve, M.; Aharony, D.; Albert, J.; Callaghan, O.; Campbell, J.; Carr, R. A. E.; Chessari, G.; Cowan, S.; Edwards, P. D.; Frederickson, M.; McMenamin, R.; Murray, C. W.; Patel, s.; Wallis, N. Application of fragment screening to the discovery of aminopyridines as inhibitors of β-secretase. *J. Med. Chem.* **2007**, *50*, 1124−1132.
(40) Geschwindner, S.; Olsson, L.-L.; Deinum, J.; Albert, J.; Edwards, P. D.; de Beer, T.; Folmer, R. H. A. Discovery of novel warheads against β-secretase through fragment-based lead generation. *J. Med. Chem.* **2007**, *50*, 5903−5911.
(41) Hyde, K. A.; Acton, E. M.; Baker, B. R.; Goodman, L. Potential anticancer agents. LXXI. Diaminopyrimidines and diamino-s-triazines related to daraprim. *J. Org. Chem.* **1962**, *27*, 1717−1722.
(42) Alker, D.; Campbell, S. F.; Cross, P. E.; Burges, R. A.; Carter, A. J.; Gardiner, D. G. Long-acting dihydropyridine calcium antagonists. 3. Synthesis and structure-activity relationships for a series of 2-[(heterocyclylmethoxy)methyl] derivatives. *J. Med. Chem.* **1989**, *32*, 2381−2388.
(43) Burtner, R. R. 2-Amino-6-aryl-5,6-dihydro-4-hydroxypyrimidines. US Patent US2748120, 1956.
(44) Vincent, S.; Grenier, S.; Valleix, A.; Salesse, C.; Lebeau, L.; Mioskowski, C. Synthesis of enzymically stable analogues of GDP for binding studies with transducin, the G-protein of the visual photoreceptor. *J. Org. Chem.* **1998**, *63*, 7244−7257.
(45) Cockerill, A. F.; Deacon, A.; Harrison, R. G.; Osborne, D. J.; Prime, D. M.; Ross, W. J.; Todd, A.; Verge, J. P. An improved synthesis of 2-amino-1,3-oxazoles under basic catalysis. *Synthesis* **1976**, 591−593.
(46) Bull, S. D.; Davies, S. G.; Garner, A. C.; O'Shea, M. D. Conjugate additions of organocuprates to a 3-methylene-6-isopropyldiketopiperazine acceptor for the asymmetric synthesis of homochiral α-amino acids. *J. Chem. Soc., Perkin Trans. 1* **2001**, 3281−3287.
(47) Patel, S.; Vuillard, L.; Cleasby, A.; Murray, C. W.; Yon, J. Apo and inhibitor complex structures of BACE (β-secretase). *J. Mol. Biol.* **2004**, *343*, 407−416.

(48) Brown, F. J.; Matassa, V. G. Preparation of heterocyclic carboxamides as leukotriene antagonists. US Patent Cont.-in-part of U.S. Ser. No. 181,455, abandoned, 1990.
(49) Boatman, S.; Harris, T. M.; Hauser, C. R. Synthesis of ketones of the type CH_3COCH_2R from acetylacetone and halides with ethanolic potassium carbonate. An alkylation-cleavage process. *J. Org. Chem.* **1965**, *30*, 3321−3324.
(50) Leslie, A. G. W.; Brick, P.; Wonacott, A. MOSFLM. *Daresbury Lab. Inf. Quart. Protein Crystallogr.* **1986**, *18*, 33−39.
(51) Bailey, S. The CCP4 suite: programs for protein crystallography. *Acta Crystallogr., Sect. D: Biol. Crystallogr.* **1994**, *D50*, 760−763.
(52) Blundell, T. L.; Abell, C.; Cleasby, A.; Hartshorn, M. J.; Tickle, I. J.; Parasini, E.; Jhoti, H. High-throughput X-ray crystallography for drug discovery. *Spec. Publ. - R. Soc. Chem.* **2002**, *279*, 53−59.
(53) Hartshorn, M. J. AstexViewerTM: a visualization aid for structure-based drug design. *J. Comput.-Aided Mol. Des.* **2003**, *16*, 871−881.
(54) Winn, M. D.; Isupov, M. N.; Murshudov, G. N. Use of TLS parameters to model anisotropic displacements in macromolecular refinement. *Acta Crystallogr., Sect. D: Biol. Crystallogr.* **2001**, *D57*, 122−133.
(55) Luellau, E.; Kanttinen, A.; Hassel, J.; Berg, M.; Haag-Alvarsson, A.; Cederbrant, K.; Greenberg, B.; Fenge, C.; Schweikart, F. Comparison of batch and perfusion culture in combination with pilot-scale expanded bed purification for the production of soluble recombinant β-secretase. *Biotechnol. Prog.* **2003**, *19*, 37−44.

JM070829P